UNIVERSITY OF CALIFORNIA, SAN DIEGO

Uridylation of microRNA-directed 5' cleavage products by TUTases

A Thesis submitted in partial satisfaction of the

requirements for the degree Master of Science

in

Biology

By

Jong Hyun Park

Committee in charge:

Professor Jens Lykke-Andersen, Chair
Professor Tracy Johnson
Professor Gene Yeo

2013

The Thesis of Jong Hyun Park is approved and it is acceptable in quality and form for publication on microfilm and electronically:

Chair

University of California, San Diego

2013

TABLE OF CONTENTS

List of Figures

ACKNOWLEDGEMENTS

I would like to first and foremost thank Professor Lykke-Andersen for giving me the opportunity to join his lab. The knowledge and experience I gained in my few years here have been invaluable.

I would also like to thank Suzanne Lee. Without her guidance and support, I would never have learned as much as I have, and I would never have accomplished as much as I did.

Next, I would like to express my gratitude to all the members of the Lykke-Andersen lab. They are awesome people.

Lastly, I'd like to thank my family for appreciating what a magnificent person I am.

ABSTRACT OF THE THESIS

Uridylation of microRNA-directed 5' cleavage products by TUTases

By

Jong Hyun Park

Master of Science in Biology

University of California, San Diego, 2013

Professor Jens Lykke-Andersen, Chair

Many studies have shown that uridylation, a post-transcriptional modification that results in the addition of non-templated uridines to the 3' ends of various RNAs, effect the stability of these transcripts. Belonging to the same family as canonical nucleotidyl transferases such as the well characterized poly(A) polymerase, non-canonical nucleotidyl-transferases (nc-rNTrs) are template-independent polymerases capapble of catalyzing the transfer of single or multiple nucleotide residues to the 3' ends of various RNAs. Here we identified the in vitro activities of six of the seven human nc-rNTrs. We found that TUTases 4 and 7 are prefer to add uridines, while TUTases 2, 3 and 5 prefer to add adenines.

Furthermore, we studied uridylation of microRNA-directed 5' cleavage products in vivo. Our preliminary results identified TUTase 2 and 7 as the enzymes that may be responsible for the uridylation of the 5' cleavage fragment. Knockdown of these enzymes in combination led to a decrease in uridylated transcripts. Here, we laid the groundwork for future experiments that will help elucidate the effects of uridylation on mRNA stability.

I.

Introduction

Overview of oligouridylation, a post-transcriptional RNA modification

The precise regulation of genes is critical for the viability of all organisms. There are multiple steps in gene expression, and each of these steps is subject to constant fine-tuning in response to various external and internal stimuli. Before proteins can be produced, genes must first be transcribed into messenger RNA. Consequently, the regulation of translation and decay of mRNA are important post-transcriptional mechanism in gene expression. RNA tailing, an RNA modification that researchers have only recently begun scrutinizing, has been linked to impacts on either the activity or stability of targeted RNAs (Norbury 2010; Wilusz and Wilusz 2008; Lee 2013; Norbury 2013). One type of tailing modification involves the addition of a short untemplated tail, composed predominantly of the nucleotide uridine, to the 3' ends of mRNAs targeted for decay. Various reports have suggested that these oligoU tails serve as a signal to recruit or activate RNA decay machinery, or, in the case of some tailed mRNAs, promote translational repression (Song, Kiledjian 2007; Hoefig 2013; Chang 2013, Lapointe 2013). A growing body of literature shows that nontemplated 3' uridylation occurs on a wide variety of RNA species in diverse eukaryotes, including mRNAs, unstable long-noncoding RNAs, pre-miRNAs and small RNAs, such as miRNAs and siRNAs (Wyman 2011; Wilusz 2012; Yates 2013). One recent report examining <200 nt long RNAs from human ESC H9 cells also uncovered transcriptional start-site associated RNAs and spliced introns as oligouridylation targets (Choi 2012). However, the mechanisms responsible for specifically recruiting and activating the enzymes that carry out RNA tailing, along with the

downstream impacts of tailing on different types of RNAs, are not well understood (Scott, Norbury 2013).

Non-canonical ribonucleotidyl transferases: RNA tailing enzymes

The enzymes capable of catalyzing RNA 3' tailing belong to the DNA polymerase-B superfamily. One prominent member of this family is the canonical nuclear poly (A) polymerase that is responsible for polyadenylating eukaryotic pre-messenger RNA. Recent studies done in different organism, ranging from ciliates and yeast to *C. elegans* and mammals, have implicated non-canonical ribonucleotidyl transferases (nc-rNTrs) in various pathways of RNA metabolism. (Martin and Keller 2007; Kwak and Wickens 2007; Schmidt and Norbury 2010). These include non-canonical poly (A) polymerases (ncPAPs) and terminal uridylyl transferases (TUTases), which are capable of catalyzing the addition of uridine residues to 3' ends of RNA. Analyses of mammalian genome sequences have revealed the existence of seven non-canonical ribonucleotidyl transferases in humans as well as in mice. Some of these have been shown to be capable of catalyzing RNA 3' tailing (Martin, Keller 2007). These enzymes are predicted to share structural homology with each other and with the canonical poly(A) polymerases that are responsible for mRNA poly(A) tail addition, but bear nucleotide recognition motifs that differ from the canonical enzymes (Figure 1). Existing studies of select family members indicate that these enzymes differ in their RNA targets, nucleotide preferences and cellular localization. Two recent structural analyses of the fission yeast cytoplasmic TUTase Cid1 found that a

conserved histidine residue in the active site was responsible for UTP selectivity over ATP (Lunde 2012; Munoz-Tello 2012; Yates 2012). Using sequence alignment of nc-rNTrs in higher eukaryotes, the authors observed that TUTases have a histidine residing in this position, while ncPAPs have an asparagine in this position (Figure 1). And indeed, mutating the histidine to asparagine in Cid1 led to a loss of UTP preference and a gain in ATP selectivity (Lunde 2012).

mGld2, the mouse homolog of human TUTase 2, has been proposed to be a poly (A) polymerase that localizes both to the cytoplasm and the nucleus (Nakanishi 2006). mGld2 extends the poly(A) tails of certain mRNAs, leading to reactivation of translation during development. Interestingly, human TUTase 2 has been implicated in mono-uridylation of pre-let-7 precursor microRNA in cultured somatic cells, in combination with TUTase 4 and TUTase 7 (Heo 2012). This mono-uridylation of the group II subset of pre-let-7 miRNAs has been reported to be required for their efficient processing and maturation into let-7 miRNA by Dicer. In addition, in human fibroblasts and mouse liver, TUTase 2/Gld2 has been implicated in the stabilization of miRNAs by monoadenylation (Katoh 2009; Burns 2011; D'Ambrogio 2012). The observation that TUTase 2 may be capable of adding an A or a U tail gives rise to further questions as to what factors determine its nucleotide specificity.

Human TUTase 3 and 5 belong to the TRF4/5 subfamily of nc-rNTRs conserved in many other eukaryotes. In yeast, Trf4p and Trf5p are the catalytic components of the TRAMP complex responsible for the 3' end addition of an oligo(A) tail. While polyadenylation stabilizes mRNA, the adenylation of

noncoding RNAs destabilizes these transcripts (Houseley 2006; Schmidt and Butler 2013). Studies in yeast have shown that aberrant noncoding RNAs are tailed by the TRAMP complex, resulting in the recruitment of the nuclear exosome (Callahan and Butler 2010). The exosome is the major 3'->5' exoribonuclease complex. Known targets of the TRAMP complex include rRNA, tRNA, sn/snoRNA, and aberrant mRNA and non-coding RNAs. TUTase 3 and 5 are homologs of Trf4p and Trf5p and are components of the human "TRAMP-like complex" in the nucleus responsible for 3' adenylation of aberrant rRNAs and certain snoRNAs (Lubas 2011, Rammelt 2011; Shcherbik 2010; Bernet 2012).

Human TUTase 4 has been implicated in histone mRNA uridylation. Experiments by Mullen and colleagues tentatively identified TUTase 1 and TUTase 3 as candidates for the oligouridylation of histone mRNA (Mullen and Marzluff, 2008). However, recent experiments indicate that knocking down TUTase 4 leads to both histone mRNA stabilization and a reduction in uridylated mRNA species, implicating TUTase 4 as the enzyme responsible for histone mRNA uridylation (Schmidt 2010; Su 2013). In addition to a role in histone mRNA decay and the aforementioned stimulation of miRNA biogenesis by mono-uridylation of group II pre-let-7, several reports, using mouse ESCs and in C. elegans, indicate that Tutase 4 oligouridylates premiRNAs bound by lin28 to repress let-7 processing by Dicer for maintanace of pluripotency (Heo 2008; Hagan 2009; Heo 2009; Lehrbach 2009; Thornton 2012). TUTase 7, which is highly related in structure to TUTase 4, has been shown to exhibit strong preference in vitro for U tailing activity over A tailing (Rissland 2007). TUTase 7 has also been shown to mono-uridylate

pre-let-7 precursor miRNA in a redundant fashion with TUTase 2 and TUTase 4 (Heo 2012), and function redundantly with TUTase 4 in the lin28-enhanced oligouridylation of pre-let-7 in mouse ESCs (Thornton et al 2012). Despite its strong homology with TUTase 4, TUTase 7 was not found to uridylate histone mRNA (Schmidt 2010). Finally, TUTase 6, also known as Star-PAP, has been shown to polyadenylate mRNAs during oxidative stress (Mellman 2008). This same enzyme is also assumed to be responsible for U6 snRNA stabilization through uridylation (Trippe 2006).

Oligouridylation and RNA repression

Pre-messenger RNA undergoes multiple processing steps before emerging as mature messenger RNA. Two important modifications are the addition of the protective 5'-7-methylguanosine cap and polyadenylation, required for the stability and active translation of mRNA (Shatkin 2000). During the process of mRNA decay, removal of the 5' cap allows degradation in the 5'->3' direction by the cytoplasmic exoribonuclease XRN1 (Parker 2004). Shortening or loss of the poly(A) tail produces an unprotected 3' end that may then be subjected to 3'->5' decay by the cytoplasmic exosome. It is important to note that these two mechanisms of decay are not mutually exclusive, and both can act simultaneously on the same transcript. In addition, activities operating at the 3' end of the mRNAs can impact decay activities imposed on the 5' end. For example, studies of the budding yeast *Saccharomyces cerevisiae* have shown that the heteroheptameric Lsm 1-7 complex is an enhancer of decapping

(Tharun 2000). The Lsm 1-7 complex binds to the short oligo(A) tails of deadenylated mRNAs and recruits the decapping complex containing Dcp1 and Dcp2, which can then remove the 5'-7-methylguanosine cap through hydrolysis (Parker 2004).

A number of proposed roles for oligouridylation in the above-described steps leading to mRNA decay have recently emerged. For example, mRNAs may undergo deadenylation-independent decapping and 5'->3' degradation in a manner dependent on uridylation by non-canonical ribonucleotidyl transferases. In the fission yeast *Schizosaccharomyces pombe*, Cid1 was found to add one or two uridines to mature, polyadenylated mRNA transcripts (Norbury 2007; Rissland 2007; Norbury 2009). In wild type cells, these U tails were found mainly on decapped transcripts. In strains deleted of the decapping factors Dcp1 and/or Lsm 1, U tails were found on capped and decapped transcripts more frequently, suggesting uridylation precedes decapping. Thus, the authors were able to conclude that uridylation is part of a novel deadenylation independent degradation pathway. In the proposed model, short U tails recruit the Lsm 1-7 complex and stimulate decapping, leading to 5'->3' decay by XRN1.

A study in *Arabidopsis thaliana* suggests that 3' uridylation may protect the 3' end of tailed RNAs from erosion by nucleases, thereby indirectly favoring degradation in the 5'->3' direction (Sement 2013). The authors identified URT1 as the uridylyltransferase responsible for uridylating oligoadenylated mRNAs. Decay assays of several mRNAs revealed that in *urt1* mutants, there were no changes in mRNA degradation rates when compared to wild type mRNAs. Furthermore, the

authors observed an increase in 3' truncated transcripts and transcripts with trimmed oligo(A) tails in *urt1* mutants. The authors hypothesize that 3' uridylation is critical for establishing the 5'->3' directionality of co-translational mRNA decay, allowing for the last ribosome to complete translation and preventing the association 3' truncated transcripts in polysomes.

In mammals, replication dependent histone mRNAs are unique among all other mRNA transcripts as they are not polyadenylated, and instead terminate in a stem-loop structure (Dominski and Marzluff 1999). Histone mRNAs are rapidly degraded at the end of S phase, or after DNA replication inhibition by treatment with hydroxyurea. Sequencing of histone mRNA decay intermediates has revealed that degradation occurs in both the 5'->3' and 3'->5' direction (Marzluff 2008). Furthermore, in both late S phase and upon DNA replication inhibition with hydroxyurea, histone mRNA degradation intermediates were found to be uridylated, though capped and decapped tailed intermediates were not distinguishable in these studies (Mullen 2008, Su 2013). SiRNA induced knockdown of the decapping factors Dcp2 and Lsm1 led to a stabilization of histone mRNA, providing further support of a model in which oligoU tails recruit the Lsm 1-7 complex and mediate decapping and 5'->3' decay (Schmidt 2011, Marzluff 2008). Additional support for oligouridylation-induced decapping through creation of an Lsm 1-7 binding site comes from an *in vitro* study using cell extracts that found that the decapping activity on synthetic RNAs is stimulated by oligoU tails, with Lsm 1-7 and decapping complex members specifically copurifying on RNAs containing oligoU tails (Song and Kiledjian 2007). The

greatest decay stimulation was observed on RNAs bearing a tail composed of 5 to 10 uridines.

A recent report proposed an alternative model for uridylation dependent histone mRNA degradation (Hoefig 2013). The authors observed that upon knockdown of the exonuclease Eri1, oligouridylated histone mRNAs accumulated in mouse embryonic fibroblasts. Eri1 was found not only to bind to histone mRNAs, but also was found to interact with Lsm1 and Lsm4. Sequencing of histone mRNAs revealed that degradation intermediates with truncated 3' stem-loops were uridylated, suggesting Eri1 degrades the 3' stem-loop structure through multiple rounds of tailing and Eri1-dependent 3->5' nuclease action. In the authors' model, the Lsm1-7 complex binds oligouridylated histone mRNAs and recruits Eri1. Then, Eri1 degrades the 3' end until it stalls at the stem-loop structure, requiring re-oligouridylation and re-recruitment of Eri1 to fully degrade the stem-loop.

Other possible roles of U tailing in mRNA metabolism involves release of uridylated transcripts from polysomes and translational repression. Multiple ribosomes translate a single mRNA simultaneously to synthesize the same protein. This cluster of ribosomes and mRNA make up a polysome, and before actively translating mRNA can be degraded, they must first be removed from the polysome. In *Aspergillus nidulans*, transcripts containing premature termination codons (PTC) were found to be tagged with a C/U tail. (Morozov 2012). Transcripts containing PTCs are rapidly degraded by the nonsense-mediated decay pathway. While mutation of cutA and cutB, the nucleotidyl

transfransferases responsible for catalyzing the addition of the C/U tails, had no effect on the steady-state levels of PTC-containing transcripts, cutA and cutB deletion strains exhibited a dramatic increase in PTC-containing transcripts bound to large polysomes. This observation supports a model where the C/U tail serves as a signal to efficiently release ribosomes from the decaying transcripts. Furthermore, in a recent study in *Xenopus laevis*, the authors found that uridylation of a polyadenylated luciferase reporter led to a significant reduction in luciferase activity, while qRT-PCR analysis revealed that there was no change in the levels of the reporter. This data supports a model where the addition of a U tail blocks the recognition of the poly(A) tail by poly(A) binding factors, preventing its ability to activate translation (Lapointe 2013).

Finally, in embryonic stem cells, the RNA binding protein Lin28 interacts with TUTase 4, resulting in the oligouridylation of pre-let-7. The addition of an oligoU tail that is 10-30 nucleotides long appears to inhibit Dicer processing of pre-let-7 and leads to pre-let-7 destruction (Heo 2009). Recent work has implicated Dis3l2, a 3'->5' exoribonuclease in carrying out the degradation of oligouridylated pre-let-7 in mouse embryonic stem cells (Chang 2013). An in vitro assay showed that Dis3l2 specifically copurifies with synthetic pre-let-7 containing a 14 nucleotide U tail but not pre-let-7 lacking a U tail. Moreover, knockdown of Dis3l2 in mouse embryonic stem cells resulted in stabilization of pre-let-7. A conserved function for Dis3l2 in catalyzing the degradation of oligouridylated mRNA transcripts has been suggested by recent work in *S. pombe* (Malecki 2013). These data suggest that the 3' oligo(U) tail in this context serves as a

signal to recruit Dis3l2 and induce 3'->5' decay of oligouridylated pre-let-7. Mutation of the Dis3l2 gene has been associated with Perlman's fetal overgrowth syndrome and a predisposition to Wilm's tumour development, suggesting that this oligouridylation-dependent degradation pathway plays critical roles in normal cell metabolism and development (Gallouzi and Wilusz 2013; Morris 2013).

Oligouridylation of 5' RISC cleavage fragments

The first report of RISC-cleavage associated oligouridylation came from studies of non-mammalian eukaryotes (Shen and Goodman 2004). In *Arabidopsis thaliana*, it was found that the 5' mRNA fragments of miRNA induced endonucleolytic cleavage by the RISC complex were oligouridylated, yielding tails of 1 to 24 nucleotides long. In the same study, oligouridylation of 5' RISC cleaved mRNA fragments was also found in mouse embryos and Epstein Barr Virus, suggesting a more widespread occurrence of RISC-fragment oligouridylation. Sequencing of these 5' mRNA fragments revealed a correlation between 3' tailing and 5'shortening, suggesting oligo(U) tails promote 5' decapping and subsequent 5'->3' degradation.

In order to study more deeply the mechanisms and consequences underlying RNA tailing in human cells, we utilized, as a potential model substrate for oligouridylation, a □-globin-based mRNA reporter with a let-7 miRNA site inserted into the 3' untranslated region. Once expressed in cultured cells, this reporter is targeted by endogenous let-7 and cleaved by the RISC complex, yielding a 5' and a 3' cleavage fragment. Unpublished data from the Lykke-

Andersen lab has suggested that the 5' fragment of this reporter is indeed uridylated (Figure 2b), demonstrating that RISC-cleaved associated RNA tailing is conserved in cultured human cells. In this study, we aimed to identify the TUTase responsible for the observed RNA tailing though a combination of biochemical assays and *in vivo* Tutase depletion by knockdown. In addition, we initiated studies into the impacts of tailing by examining impacts on the steady state level of our reporter upon TUTase knockdown.

II.

Results

Uridylation of the 5' fragment of RISC cleaved mRNA occurs in cultured human cells

Cell culture experiments were done in human HeLa Tet-Off cells. The □-globin reporter containing a let-7 miRNA site (Bwt let-7) was transiently transfected into the cells. We used adapter-ligation mediated reverse transcription-PCR (aIRT-PCR) to detect the 5' RISC cleavage fragment on an ethidium bromide stained agarose gel. In this method, an adaptor is ligated to the 3' ends of total RNA, and the Bwt let-7 reporter is specifically amplified by RT-PCR using a gene specific forward primer and adapter specific RT and reverse primers (Figure 2a). During the reverse transcription step, two different primers were used. An "unbiased" primer bearing a sequence complementary to the adapter was used to reverse transcribe all transcripts, while a U-specific primer bearing sequence complementary to the adapter, as well as three 3' dA residues was used to reverse transcribe transcripts containing a minimum of three terminal U residues. Using unbiased primer, we were indeed able to detect the full length Bwt let-7 reporter and the 5' RISC cleavage fragment (Figure 2b, upper panel). We were also able to detect uridylated transcripts using the U-specific RT primer (Figure 2b, lower panel).

In vitro activity assays establish nucleotide preferences of the human non-canonical ribonucleotidyl transferases

The in vitro tailing reactions used in this study were designed to measure 3' tailing activity on a provided 20 nt single standed RNA substrate predicted to

bear minimal secondary structure, $CA_{(10)}$. Six of the seven nc-rNTrs, TUTase 2-7, were purified from HEK 293T FITR cells stably expressing 3x Flag tagged TUTases. To normalize the concentrations of each protein preparation used in tailing reactions, a GST-Flag protein of known concentration acted as an estimation standard on anti-Flag Western blots. Figure 3a is an example of a Western blot used to normalize TUTase concentration levels. Note that GST-Flag runs in the gel at a size of approximately 27 kDa. In the nc-NTr preparations shown, TUTase 6 and 7 were determined to purify at a concentration of 37.5 ng/µl relative to GST-Flag, while TUTase 2, 3, 4, and 5 were found to be 25 ng/µl relative to GST-Flag. The bands at approximately 25 kDa in the TUTase 2, 3 and 6 samples most likely correspond to the 3X Flag peptide present in the elution buffer.

In order to estimate the approximate absolute concentration of purified proteins used in the activity assays, silver staining analysis was utilized. The levels of purified TUTase 4 was compared to a known quantity of BSA standard (figure 3b). Based on this data, we were able to conclude that each reaction contained a protein concentration of approximately 150 nM.

It was anticipated that any co-purifying RNAs present in the nc-rNTr preparation could give rise to a tailed reaction product, thereby complicating the interpretation of the results. To address this possibility, Tutase 4 and Tutase 7 were purified from cell lysates prepared in the presence or absence of RNase A. To further examine the dependence of the signal on our synthetic RNA substrate, tailing reactions were also carried out in the presence or absence of the RNA substrate. As shown in Figure 4, no co-purifying endogenous RNA(s) were tailed

with untreated TUTase 4. Copurifying endogenous RNA(s) were tailed by TUTase 7, but these RNAs were efficiently removed with RNase A treatment. Thus, all subsequent tailing reactions described here were performed with RNase A treated TUTase preparations.

Under physiological conditions found in human cells, ATP is present at a 10-fold higher concentration than CTP, GTP, and UTP (Traut 1994). In order to examine nucleotide preference under relatively physiological nucleotide concentrations in the tailing reactions, ATP was provided at a concentration of 0.5 mM, while CTP, GTP and UTP were provided at 0.05 mM. In Figure 5, the *in vitro* tailing activities of human Tutases 2-7 were compared. Tutase 1, known to localize to mitochondria, was omitted from this study (Nagaike et al. 2005). TUTases 2, 3, and 5 exhibited preferential monoadenylation activity (Figure 3a). TUTase 2 is also capable of adding a single G to the RNA substrate, but the signal observed for this activity was at a lower level, indicating a lesser preference for this nucleotide. TUTase 4 and 7 exhibited much stronger overall activity, with a preference for mono-U and oligo-U tailing (Figure 5b). Moreover, the lengths of these tails extended well beyond 300 nucleotides. TUTase 4 and 7 also have the capability of incorporating A's and C's, but at a lower level compared to U-addition. TUTase 7 tailing yielded a larger accumulation of long tailed over short tailed substrates, while TUTase 4 favored the addition of shorter tails. Nonetheless, TUTase 4 was still capable of creating long tails, albeit at a lower efficiency than TUTase 7. A darker exposure of Figure 5b revealed the mono-adenylation and

mono-uridylation activities of TUTase 6 (Figure 5c). As a negative control, reactions containing the 3x Flag tag alone were included.

Figure 4 shows the results of tailing reactions of Tutases 2-7 under single nucleotide conditions. Only a single nucleotide was added to each reaction, as opposed to all four nucleotides, in order to assess absolute capabilities to tailing with different nucleotides. Similar to what was seen under physiological nucleotide concentrations, TUTase 2, 3 and 5 prefer to add mono-A tails to the RNA (Figure 6a). However, all the TUTases are able to use a broader range of nucleotides in RNA tailing under single nucleotide conditions. TUTase 2, 3 and 5 were now able catalyze mono-C, -U and –G addition. TUTase 4 and 7 displayed the same pattern of short and long U tailing as was seen under physiological nucleotide conditions (Figure 6b). Moreover, TUTase 7 showed weaker activity than TUTase 4, but retained a stronger long-tailing activity relative to short-tailing. TUTase 4 exhibited strong short- and long-tailing with UTP, but added only short tails with ATP and CTP. Note that the weaker Tutase 7 activity observed in Figure 6b could be due to technical error in performing the experiment, as the TUTase 7 preparation used in this experiment underwent an additional freeze-thaw cycle, which may have resulted in activity loss.

Because TUTase 7 displayed the stronger poly(U) polymerase activity compared to Tutase 4, a time course was used to study the activity rates of short and long tailing (Figure 7). In a 45 minute reaction, time points were taken every 9 minutes. Short and long tailed RNA substrates appeared in as early as 9 minutes. While the accumulation of short tailed products was not observed to

increase over the course of 45 minutes, the amount of long tailed species increased dramatically over the time course. Together, the data presented in Figures 4 and 5 are consistent with a model in which Tutase 7 has two modes of activity: mono/oligo uridylation and relatively slower poly-nucleotide (likely U-rich) polymerization that is stimulated by a short (1-3) U-containing tail.

Knockdown of TUTase 2 and 7 in combination results in a decrease in the overall levels of oligo(U) tailing of the 5' RISC cleavage fragment.

Next we undertook experiments aimed at identifying the TUTases responsible for tailing the 5' RISC-cleaved fragment. Based on our *in vitro* activity assay results above, TUTase 4 and TUTase 7 were predicted to be the most likely candidates. In light of a recent study implicating TUTase 2, 4 and 7 as the enzymes responsible for mono-uridylating pre-let-7 precursor miRNA, we also included TUTase 2 in our analysis (Heo et al. 2012). The study found that TUTase 2, 4 and 7 act in a redundant fashion, and therefore, we hypothesized that this could be occurring in the case of 5' RISC-cleaved and tailed fragments.

Using unbiased al-RT-PCR, we were able to clone and sequence the 3' ends of the 5' RISC cleavage fragment of our Bwt let-7 reporter. A schematic of the cleavage site is shown in figure 8a. Cleavage occurs between nucleotides 654 and 655 of the reporter. AlignX® was used to align sequences against the Bwt let-7 reporter (figure 8b). The dinucleotide barcode and the four nucleotide randomer following it insure that any two similarly tailed fragments can be identified as either two unique species containing the same tail or two duplicates

arising from PCR amplification. In the absence of a knockdown, nearly 60% of reads were tailed. And of these tailed reads, only 20% were single nucleotide tails; 80% of the tails were longer than one nucleotide (figure 8c). The average length of a tail was 4.5 nucleotides (figure 8e). Over 90% of the nucleotides incorporated into tails were uridines (figure 8d), and 20% of the tails were added at nucleotide 654 of the 5' RISC cleavage fragment, which corresponds with the cleavage site (figure 8f).

The three candidate TUTases were knocked down, both alone and in combination, by siRNAs, and the effects on tailing of the Bwt let-7 reporter were observed by sequencing. The Western blots in Figure 8f display the levels of depletion achieved with each knockdown condition. TUTase 2 was knocked down to approximately 11%, TUTase 4 was knocked down to less than 11%, and TUTase 7 was knocked down to between 33% and 11%. Upf1 served as a loading control, while luciferase siRNA served as a negative control. Upon knockdown of TUTase 2 and 7 in combination, the percentage of tailed transcripts was reduced. This can be seen in the TUTase 2/7 combination knockdown and the TUTase 2/4/7 combination knockdowns, with no additional impact of inclusion of Tutase 4 in the triple knockdown (Figure 8c). Analysis of the nucleotide compositions of the tails under TUTase knockdown conditions did not reveal any significant differences. Detected tails were almost exclusively composed of uridine residues (figure 8d). Analysis of the average tail lengths of tailed species revealed that all TUTase knockdown conditions shortened the average tail length, with TUTase 2 knockdown having the most dramatic effect (figure 8e).

The lengths of tails range from 1 to over 10 nucleotides long (figure 8f). Combination knockdowns of TUTase 2/7, TUTase 4/7 and TUTase 2/4/7 along with a single TUTase 4 knockdown all led to an increase in mono-tailed transcripts. Interestingly, any combination knockdown conditions of TUTase 2, 4 and 7 led to a decrease in the occurrence of full length transcripts that were 654 nucleotides long (figure 8g). Higher levels of truncated transcripts that were 653 nucleotides long were seen instead. This effect can also be seen when only looking at tailed (figure 8h, top panel) or untailed transcripts (figure 8i, top panel). On the other hand, single knockdowns of either TUTase 2, 4 or 7 alone resulted in an increase in the occurrence of full length transcripts when, regardless of whether they contained a tail or not (figure 8g).

TUTase 7 associates preferentially with the 5' RISC cleavage fragment over full-length Bglobin-let7 mRNA

A biochemical approach was also used to implicate the TUTase responsible for tailing the 5' RISC cleavage fragment which involved looking for a physical interaction between the mRNA fragment and the tailing machinery. In a preliminary experiment, transiently expressed TUTase 4 and 7 were immunopurified from HEK293T cells and examined for copurifying Bwt let-7 reporter. In addition to the wild type TUTases, catalytically inactive mutants were made for inclusion in the experiment (figure 9a). These mutants have two aspartate residues in the catalytic domain mutated to alanine residues, thereby inactivating their ability to catalyze the addition of nontemplated nucleotides to

RNA substrates (Norbury 2007). Our own In vitro tailing assay shows that the tailing activity of the catalytically dead mutants is severely hindered when compared to the wild type TUTases (figure 9b). Our hypothesis was that these catalytically dead "DADA" mutants might be stabilized in association with their RNA targets, stalled in release due to a lack of necessary activity. Therefore, if a physical interaction did exist between the TUTase and the reporter, we would expect to see increased signal with a catalytically inactive mutant versus a wild type TUTase.

Significant signal for the B-let7 reporter was observed only in the Tutase 7 purifications. In the case of TUTase 4, an interaction with the full length Bwt let-7 reporter was only weakly detectable with the DADA mutant (figure 9c); however, in this preliminary experiment, protein recovery in the IP was not measured, making the significance of the observed interaction unclear. In the case of TUTase 7, signal corresponding to the full length reporter can be seen for both the wild type and DADA mutant. Interestingly, the data reveals an enriched interaction between TUTase 7 DADA and the 5' RISC cleavage fragment, over the full-length mRNA reporter and relative to TUTase 7 WT. In a biological repeat of this experiment, the TUTase 7 DADA mutant once again showed a higher affinity for the 5' RISC cleavage fragment over the full-length mRNA than the wild type version (figure 9d). Western blot data in figure 9e reveals that, in this experiment, TUTase 7 DADA was expressed at a much lower level than wild type, which may explain the weaker signal observed in the TUTase 7 DADA lane

(figures 9c and 9d). These data further support that TUTase 7 is directly involved in the tailing of the 5' RISC cleavage fragment.

TUTase knockdowns yielded minimal impacts on steady state levels of Bwt let-7 reporter

Northern blot analysis was used in order to measure the steady state levels of Bwt let-7 mRNA. We were able to detect both the full length and the 5' RISC cleavage fragment using a probe antisense to exons 1 and 2 of Bwt mRNA (PC Delta 1,2) (Figure 10a). This probe also detects our stable transfection control, Bwt Gap 3'UAC mRNA. A biological repeat of the experiment was probed with the PTS(2) probe, which detects all three mRNAs (Bwt Gap 3'UAC, Bwt let-7 full length, and 5' RISC cleavage fragment) by hybridizing to the 3' UTR regions (Figure 10e).

Based on our preliminary sequencing data, we anticipated an impact on the metabolism of the 5' RISC-cleaved fragment upon a knockdown of TUTase 2 and 7 in combination. Given an implicated role in RNA decay for oligouridylation, we first looked for changes in the steady state levels of the Bwt let-7 mRNA. A recent report observed that knockdown of TUTase 2, 4 and 7, either alone or in combination, led to an increase in the levels of group II pre-let-7 precursor miRNAs and a decrease in mature let-7 levels and repressive function (Heo et al. 2013). Because the cleavage of our reporter is dependent on let-7 miRNA, a reduction in cleavage efficiency is expected under TUTase 2, 4 and 7

knockdown conditions and can be monitored by an increase in the levels of the full length reporter relative to the transfection control, Bwt Gap 3'UAC.

To detect changes in the stability of the 5' RISC cleaved fragment, we quantified the ratio of the 5' RISC cleavage fragment to the total levels of Bwt let-7 mRNA (5' RISC cleavage fragment signal over 5' RISC cleavage fragment signal plus full length signal). Any changes to this ratio when comparing TUTase knockdown conditions to the luc siRNA control would be expected to be due to a change in the levels of cleavage, giving rise to more or less 5' fragment if cleavage is stimulated or inhibited, respectively, or due to a change in the stability of the 5' RISC cleavage fragment.

With the exception of an increase in full length Bwt let-7 levels under TUTase 7 depletion, no significant or consistent impacts were observed for either the full length or 5' RISC cleaved Bwt-let-7 reporter mRNAs (Figures 10b and 10c). These data suggest that in our Hela Tet-Off cells, only TUTase 7 depletion reduced let-7 levels to a degree that reduced cleavage.

The repeat experiment (Figure 10e) included XRN1 and Lsm1 knockdowns. Under both these conditions, we anticipated a stabilization of the 5' RISC cleavage fragment if the role of oligouridylation in 5' RISC-cleaved fragment degradation is to recruiting the Lsm 1-7 complex and thus mediating decapping and Xrn1-dependent 5'->3' decay, as suggested in previous studies of unstable oligouridyated transcripts in other systems. Curiously, our preliminary results suggest that Xrn1 depletion actually stimulates cleavage, which interferes with our ability to distinguish increased cleavage from an increase in 5' RISC fragment

stability in these steady state assays (Figures 10f and 10g). LSM1 depletion did indeed result in increased relative 5' RISC fragment levels without impacting cleavage, consistent with our predictions.

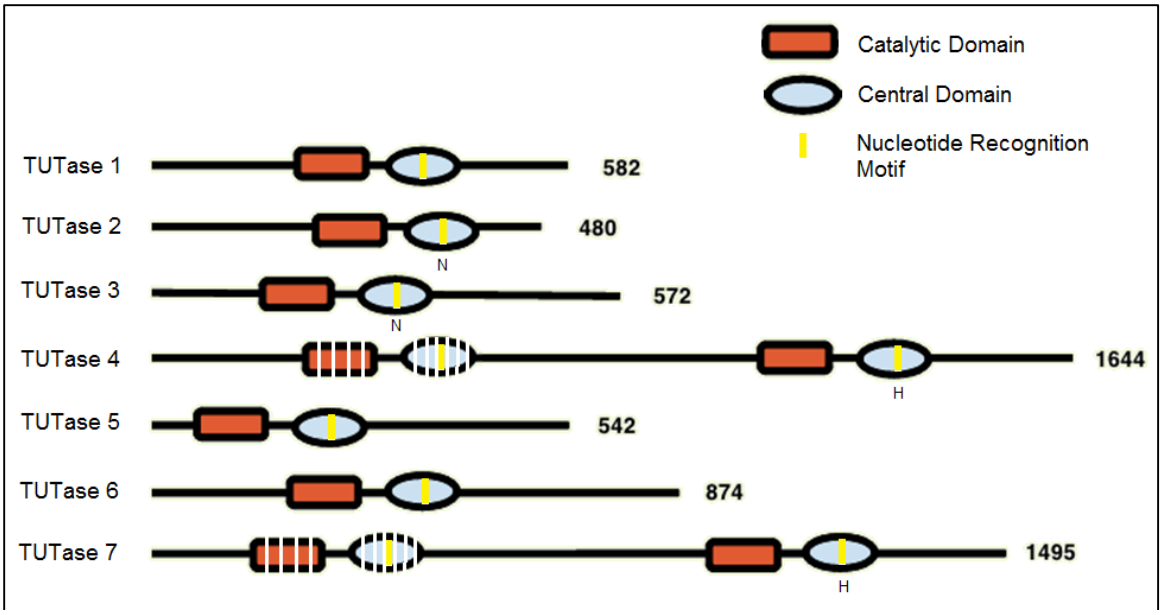

Figure 1. There are seven human non-canonical ribo-nucleotidyl transferases
Schematic showing the 7 human TUTases and their domains. The letters H and N under the nucleotide recognition motif stand for histidine and asparagine respectively. The N terminal domains of TUTase 4 and 7 are predicted to be inactive.

A

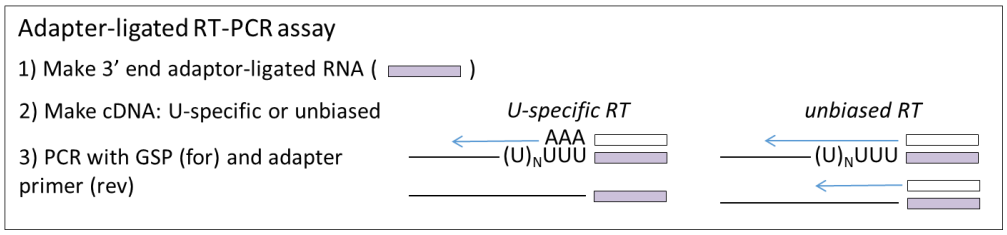

B

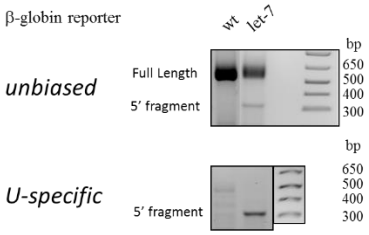

Lee, unpublished data

Figure 2. Uridylation of the 5' RISC cleavage fragment of Bwt let-7 mRNA can be detected by al-RT-PCR

(A) Schematic of al-RT-PCR
(B) Ethidium bromide stained agarose gel showing bands corresponding to the full length reporter and the 5' RISC cleavage fragment. The U specific RT primer is able to detect uridylated 5' RISC cleavage fragment.

Figure 3. Estimation of the relative concentration levels of TUTases used in the in vitro tailing assays

(A) Western blot comparing concentrations of protein purifications to GST-Flag. GST-Flag runs at approximately 27 kDa. A titration from 125 ng/µl to 12.5 ng/ µl was used to assign relative concentrations to the purified TUTases. 1 µl of the TUTase purifications was loaded into each lane.
(B) Silver stained protein gel comparing levels of protein purifications to a BSA standard of known quantity.

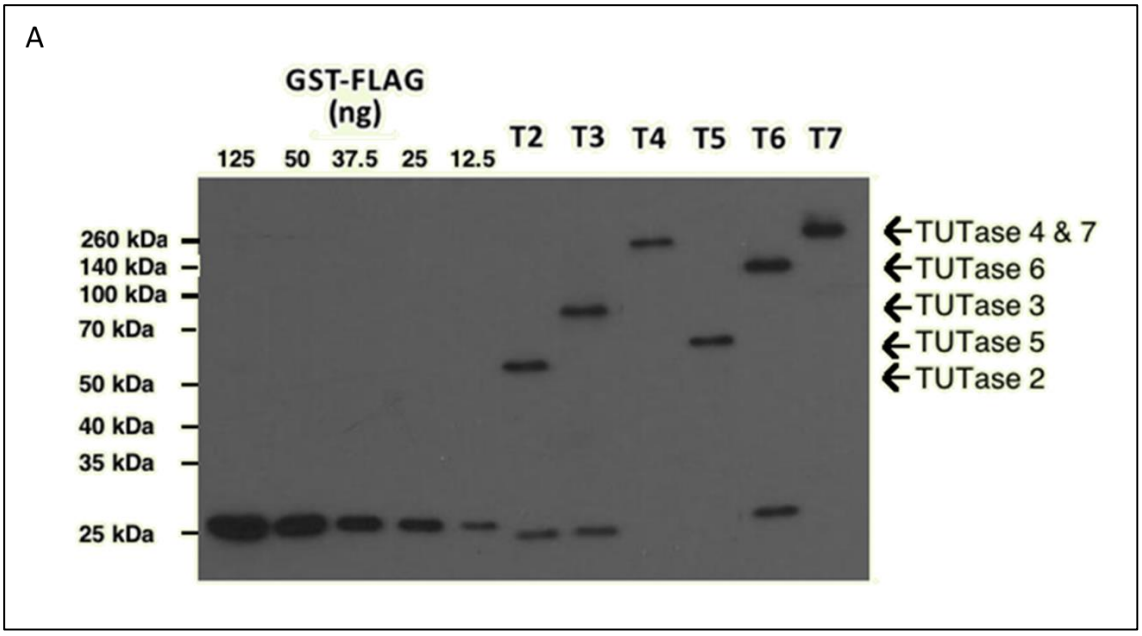
A
GST-FLAG (ng)
125
50
37.5
25
12.5
T2
T3
T4
T5
T6
T7
260 kDa
140 kDa
100 kDa
70 kDa
50 kDa
40 kDa
35 kDa
25 kDa
TUTase 4 & 7
TUTase 6
TUTase 3
TUTase 5
TUTase 2

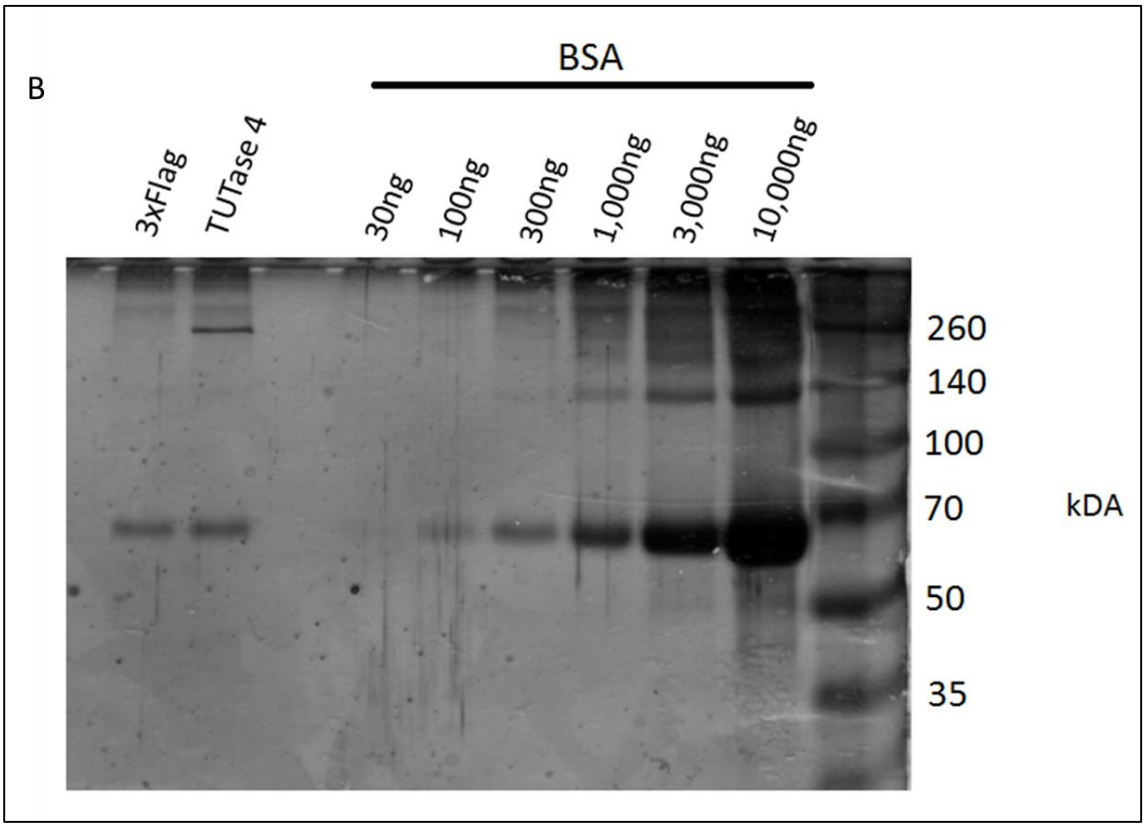
B
BSA
3xFlag
TUTase 4
30ng
100ng
300ng
1,000ng
3,000ng
10,000ng
260
140
100
70
50
35
kDA

Figure 4. RNase A treatment on cell lysates during protein purifications is sufficient to remove any endogenous RNA(s) pulled down with the proteins.

(+) for RNase A indicates the presence of RNase A during nc-rNTr purification, while a (-) indicates the absence of RNase A in untreated purifications. (+) for RNA substrate indicates the presence of the synthetic (CA)10 oligonucleotide RNA substrate in the tailing reaction. The large arrow indicates the size of the full length RNA substrate.

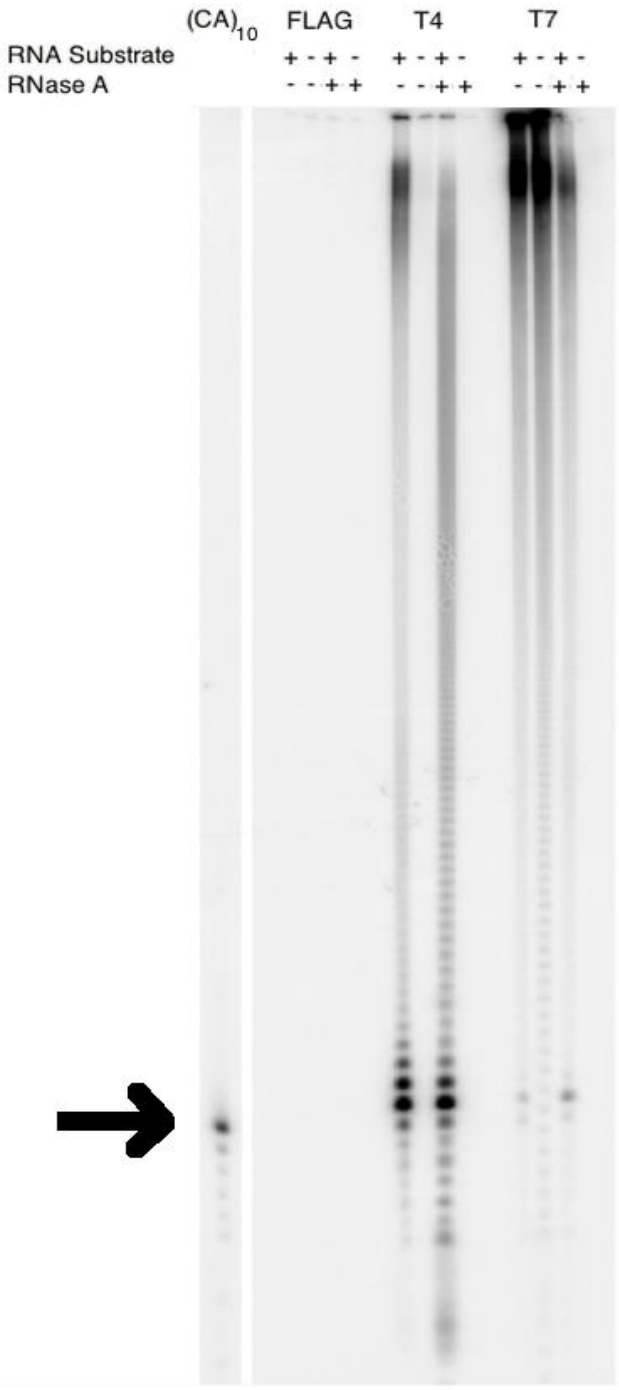
(CA)10
FLAG
T4
T7
RNA Substrate
RNase A
+ - + - + - + - + - + -
- - + + - - + + - - + +

Figure 5. The human nc-rNTrs exhibit different nucleotide preferences, activity strengths, and product tail lengths under physiological NTP conditions.

The letter directly above each lane corresponds to the radioactive nucleotide added to the tailing reaction. (a) TUTase 2, 3 and 5 add only a single nucleotide tail with a preference for ATP. (b) TUTase 4 and 7 prefer to add long U tails, but are capable of A- and C-addition. (c) A darker exposure of Figure 3a. (d) A darker exposure of Figure 3b shows that TUTase 6 is capable of adding a single A or U tail.

A

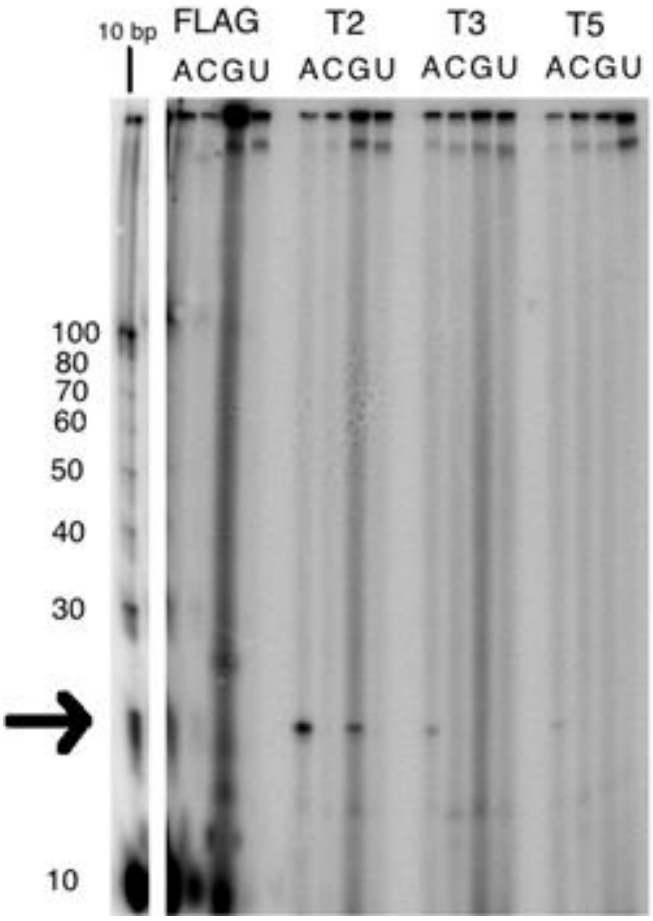

B

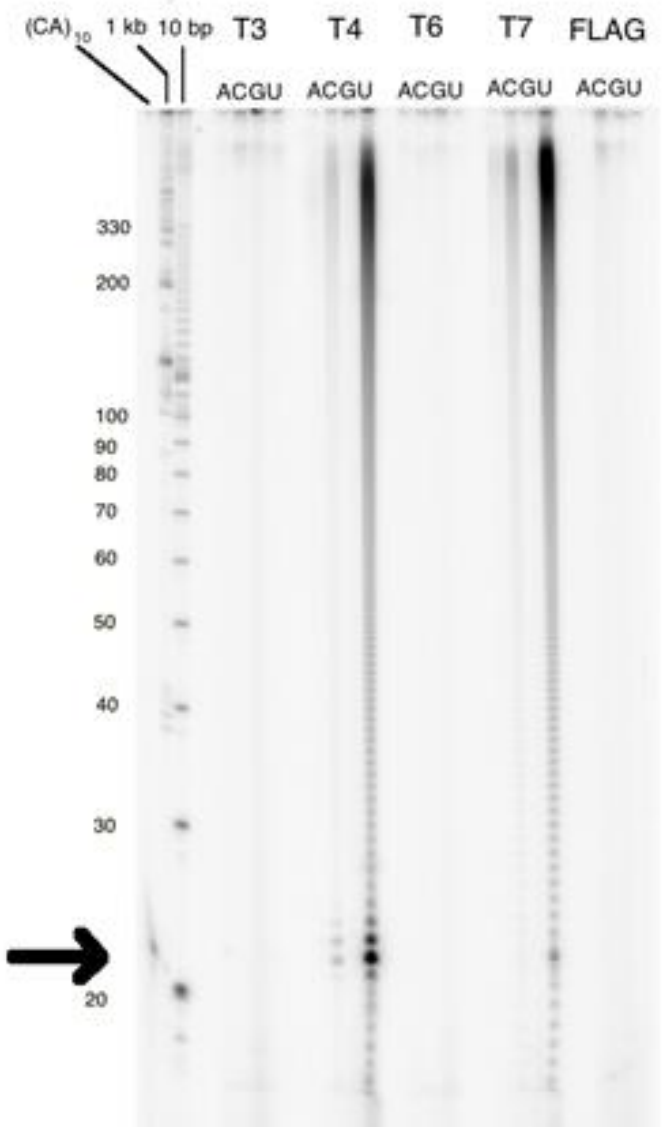

Figure 5. The human nc-rNTrs, Continued

C

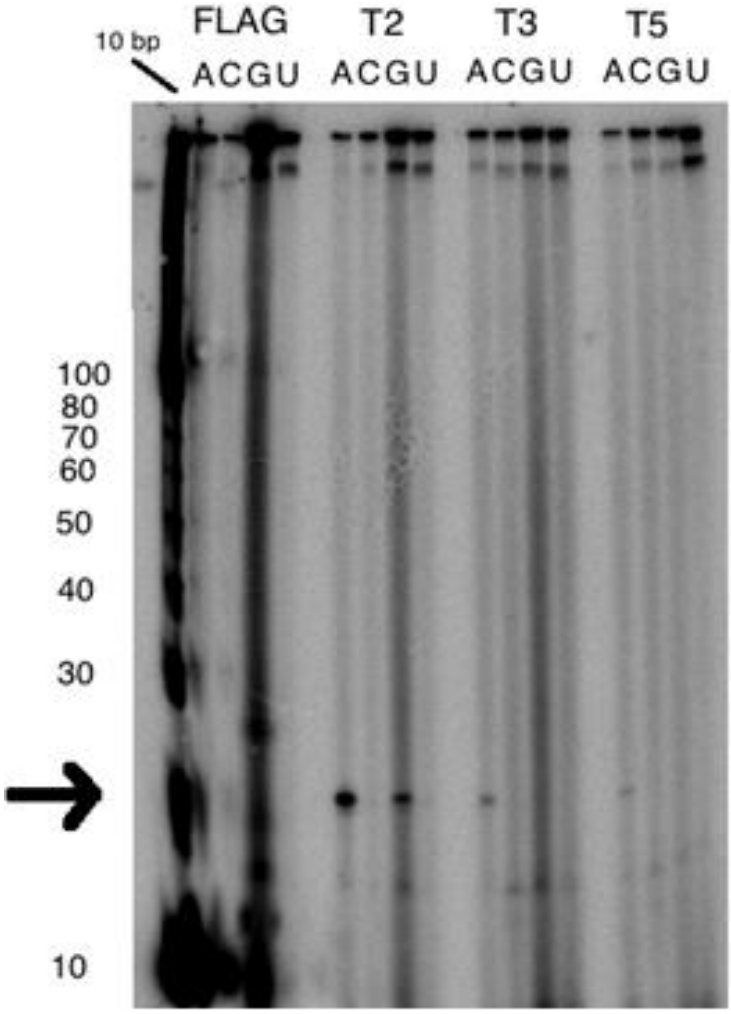

Figure 5. The human nc-rNTrs, Continued

D

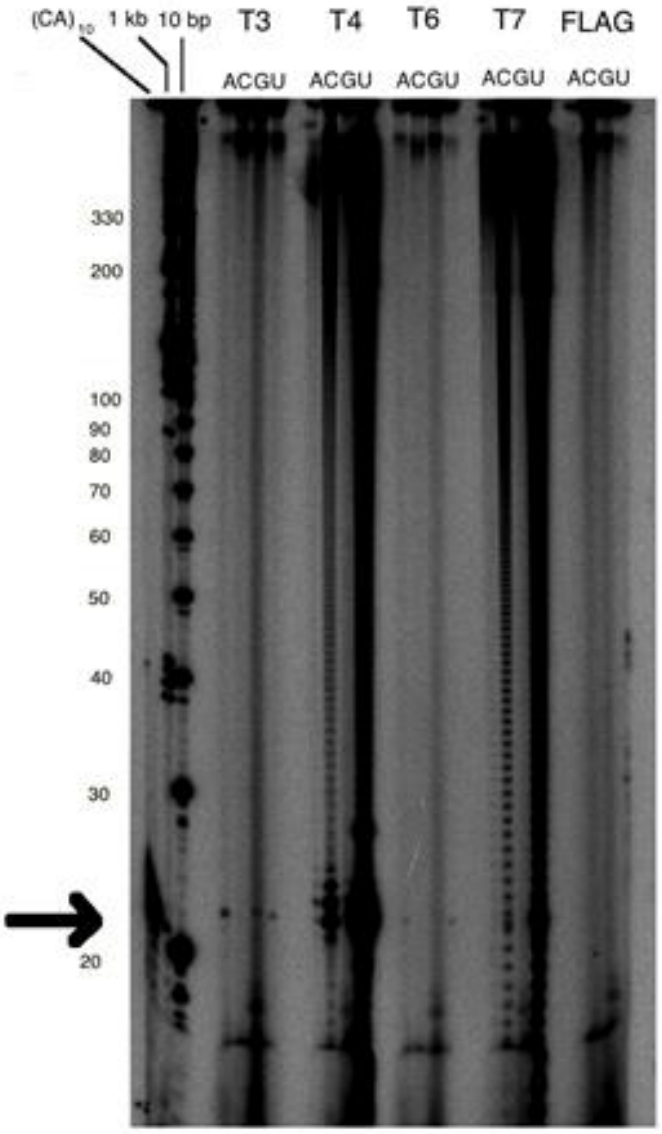

Figure 5. The human nc-rNTrs, Continued

Figure 6. Under single NTP conditions, TUTases still exhibit distinct nucleotide preferences, yet are capable of broader nucleotide use in RNA tailing.

The letter directly above each lane corresponds to the only nucleotide present in the reaction. (a) TUTase 2, 3 and 5 can use all four nucleotides in tailing. Tails continue to be only 1 nucleotide in length. Nucleotide preference remains the same as in physiological nucleotide conditions. (b) TUTase 4 is capable of catalyzing the addition of all four nucleotides to the RNA substrate. It is exceptionally efficient with UTP and can catalyze long oligo-U tails in addition to short U tails. TUTase 7 is only capable of U-tailing, and prefers long tailing activity to short tailing. (c) A longer exposure of a. (d) A longer exposure of b.

A

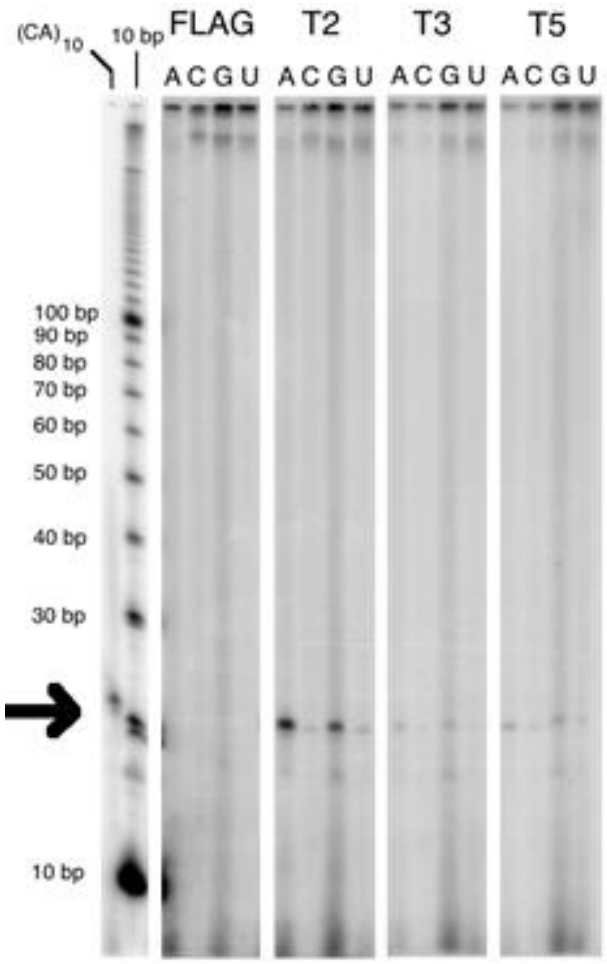
(CA)10
10 bp
FLAG
T2
T3
T5
A C G U A C G U A C G U A C G U
100 bp
90 bp
80 bp
70 bp
60 bp
50 bp
40 bp
30 bp
10 bp

B

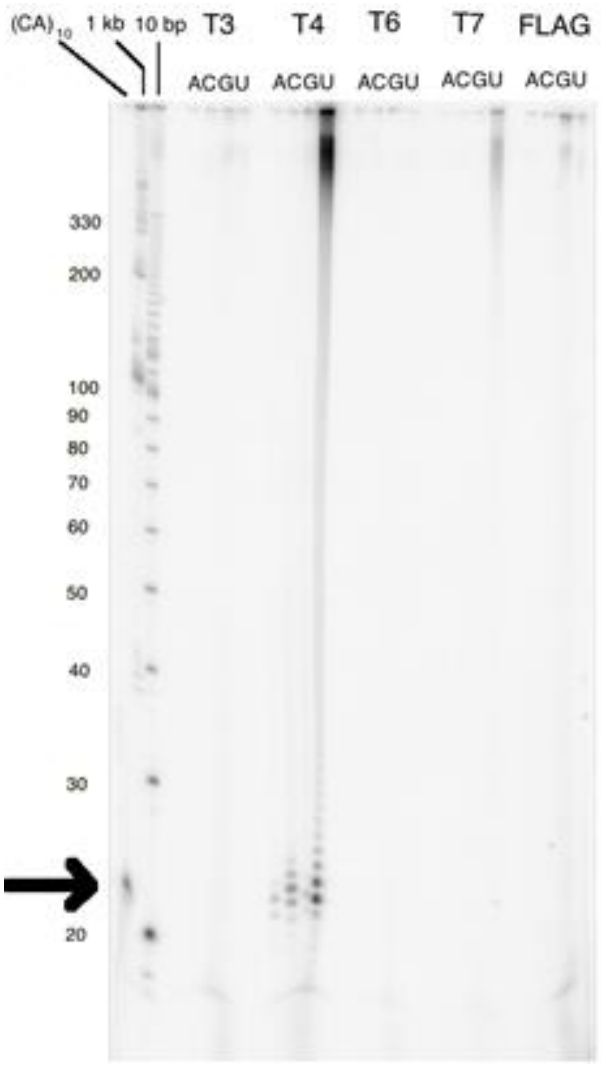

Figure 6. Under single NTP conditions, Continued

C

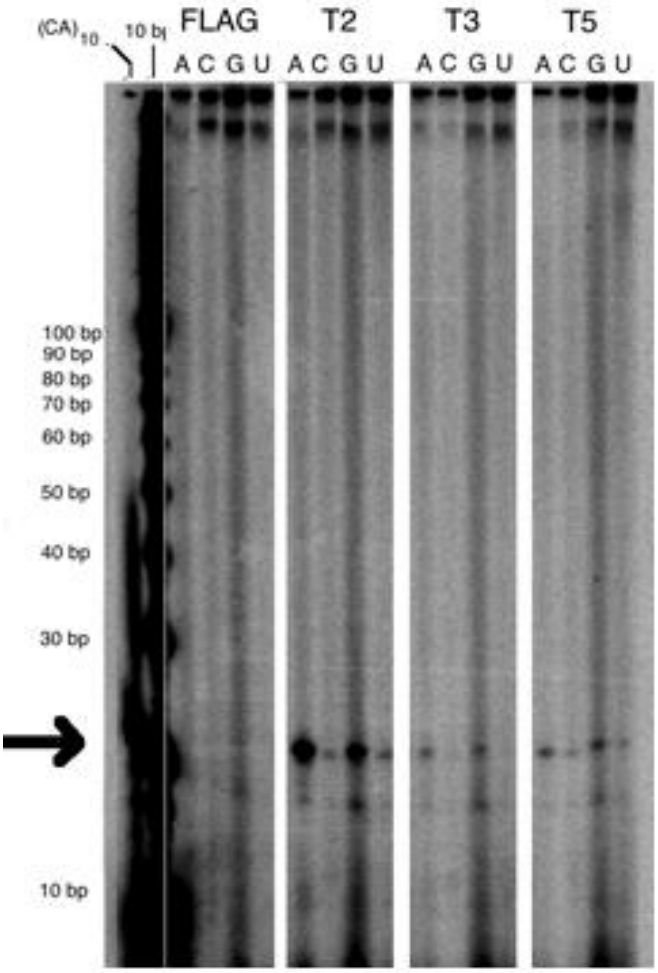

Figure 6. Under single NTP conditions, Continued

D

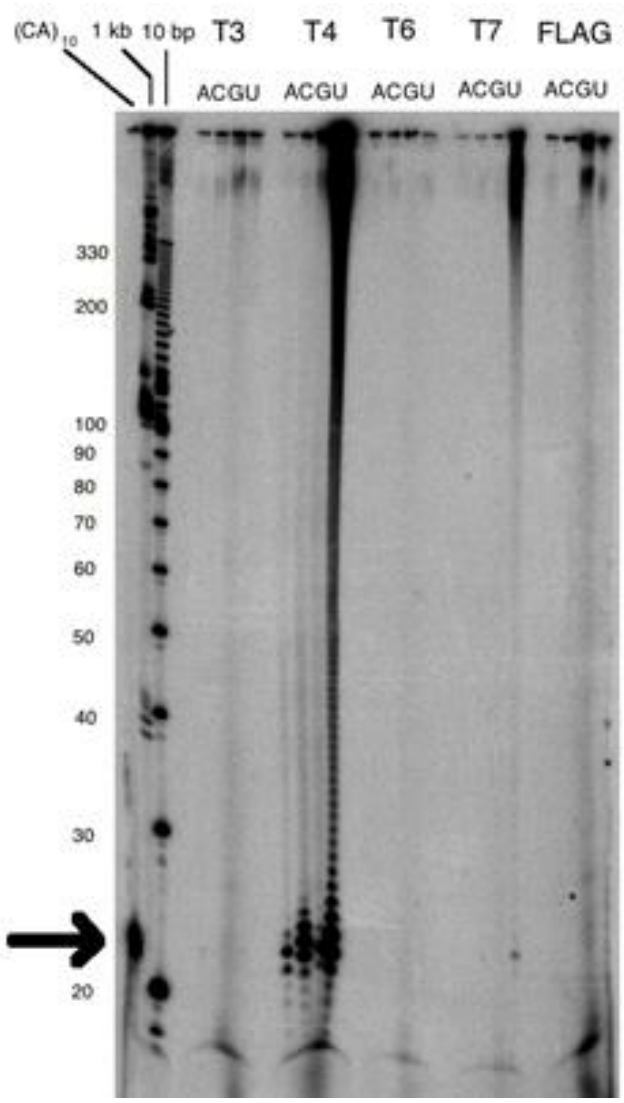

Figure 6. Under single NTP conditions, Continued

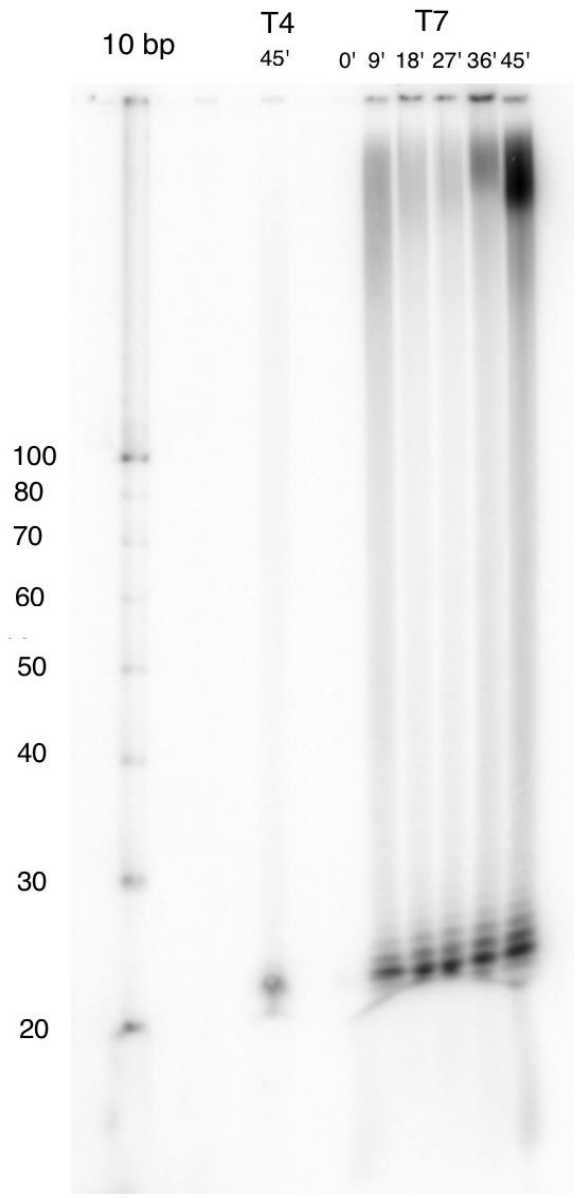

Figure 7. TUTase 7 exhibits relatively robust oligo/poly(U) polymerase activity.

A 45' time course with 6 time points was done under physiological NTP conditions with radioactive UTP. Long tailed substrates start to rapidly accumulate starting at approximately 36' minutes into the tailing reaction, while the amount of short tailed substrates remains relatively constant.

Figure 8. Sequencing of the 3' ends of the 5' RISC cleavage fragment of Bwt let-7 mRNA.

(A) Schematic of the Bwt let-7 reporter. The reporter is cleaved by let-7 miRNA, giving rise to a 5' and a 3' cleavage fragment. Cleavage occurs at nucleotide 654 of the reporter.
(B) AlignX® alignment showing dinucleotide barcode and the four nucleotide randomer.
(C) Graph plotting out all sequencing reads. Each read was sorted into one of three groups: reads with no tail, reads with a 1 nucleotide tail, and reads with >1 nucleotide tail
(D) Analysis of nucleotide tail composition. Only reads that were tailed are included.
(E) Graph plotting average length of tails. Only reads that were tailed are included.
(F) Graph plotting out the distribution of the tail lengths. The length of the tails are represented by the X-axis, while the percentage of the total reads of each siRNA treatment condition are represented by the Y-axis.
(G) The lengths of the 5' RISC cleavage fragment are plotted here. All transcripts have been included, both tailed and untailed.
(H) The lengths of the 5' RISC cleavage fragment of only tailed transcripts are plotted here. The knockdown conditions are grouped into three graphs. Conditions containing a TUTase 2 knockdown are found on the upper graph, TUTase 4 knockdowns are found on the middle graph, and TUTase 7 knockdowns are found on the lower graph.
(I) The lengths of the 5' RISC cleavage fragment of only untailed transcripts are plotted here. The knockdown conditions are grouped into three graphs. Conditions containing a TUTase 2 knockdown are found on the upper graph, TUTase 4 knockdowns are found on the middle graph, and TUTase 7 knockdowns are found on the lower graph.
(J) Western blot showing levels of TUTase knockdowns. UPF1 was used as a loading control.

A

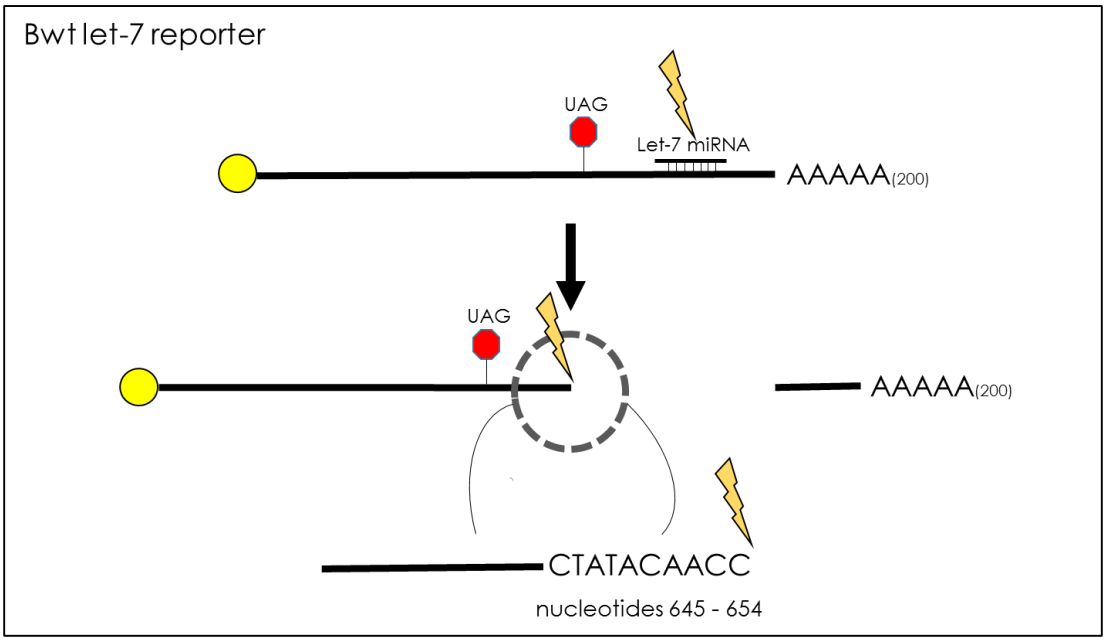
Bwt let-7 reporter
UAG
Let-7 miRNA
AAAAA(200)
UAG
AAAAA(200)
CTATACAACC
nucleotides 645 - 654

B

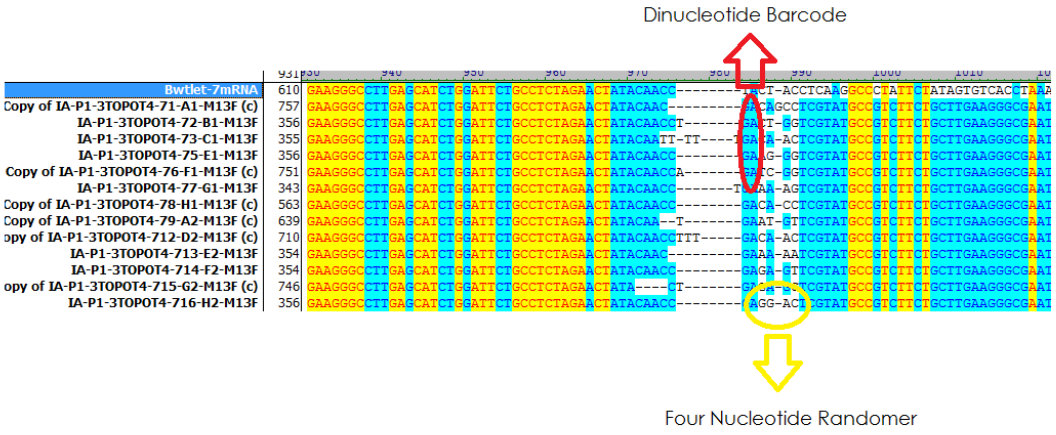
Dinucleotide Barcode
Four Nucleotide Randomer
Bwtlet-7mRNA
Copy of IA-P1-3TOPOT4-71-A1-M13F (c)
IA-P1-3TOPOT4-72-B1-M13F
IA-P1-3TOPOT4-73-C1-M13F
IA-P1-3TOPOT4-75-E1-M13F
Copy of IA-P1-3TOPOT4-76-F1-M13F (c)
IA-P1-3TOPOT4-77-G1-M13F
Copy of IA-P1-3TOPOT4-78-H1-M13F (c)
Copy of IA-P1-3TOPOT4-79-A2-M13F (c)
opy of IA-P1-3TOPOT4-712-D2-M13F (c)
IA-P1-3TOPOT4-713-E2-M13F
IA-P1-3TOPOT4-714-F2-M13F
opy of IA-P1-3TOPOT4-715-G2-M13F (c)
IA-P1-3TOPOT4-716-H2-M13F

C

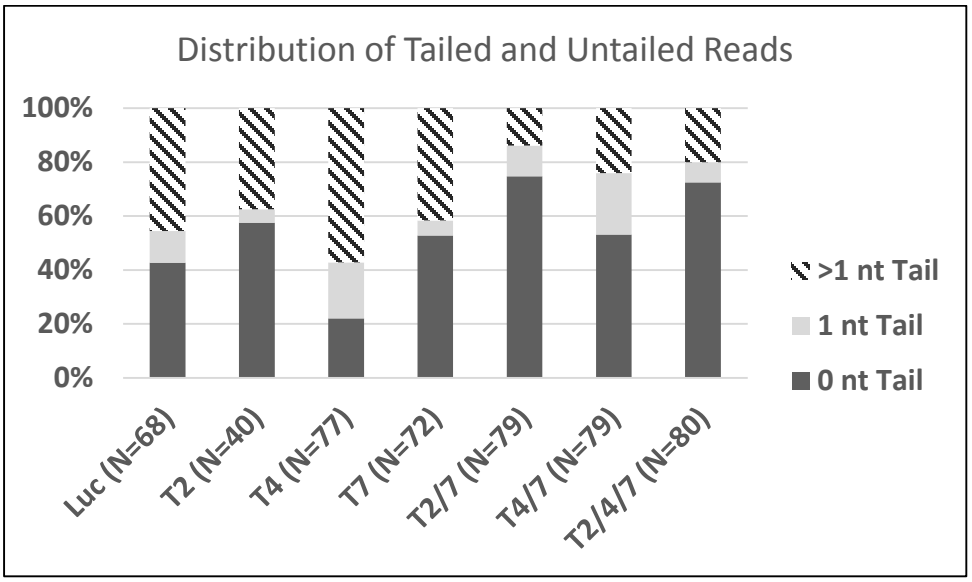

D

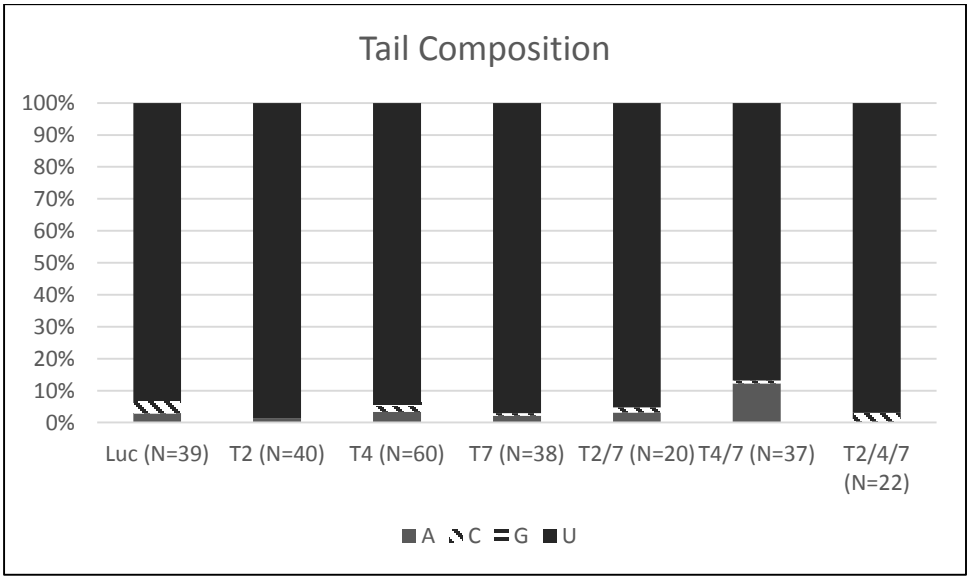

Figure 8. Sequencing of the 3' ends, Continued

E

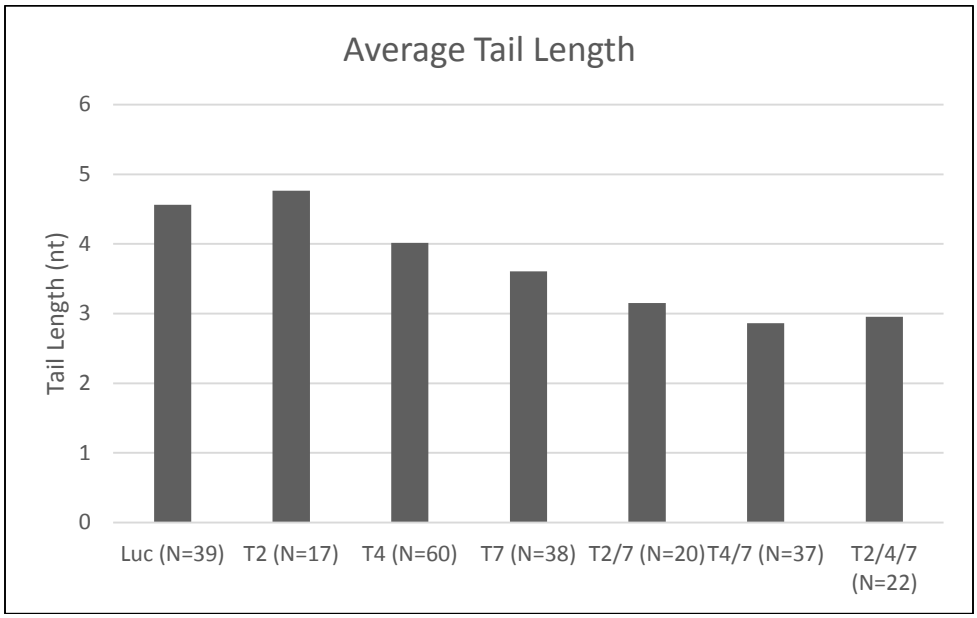

F

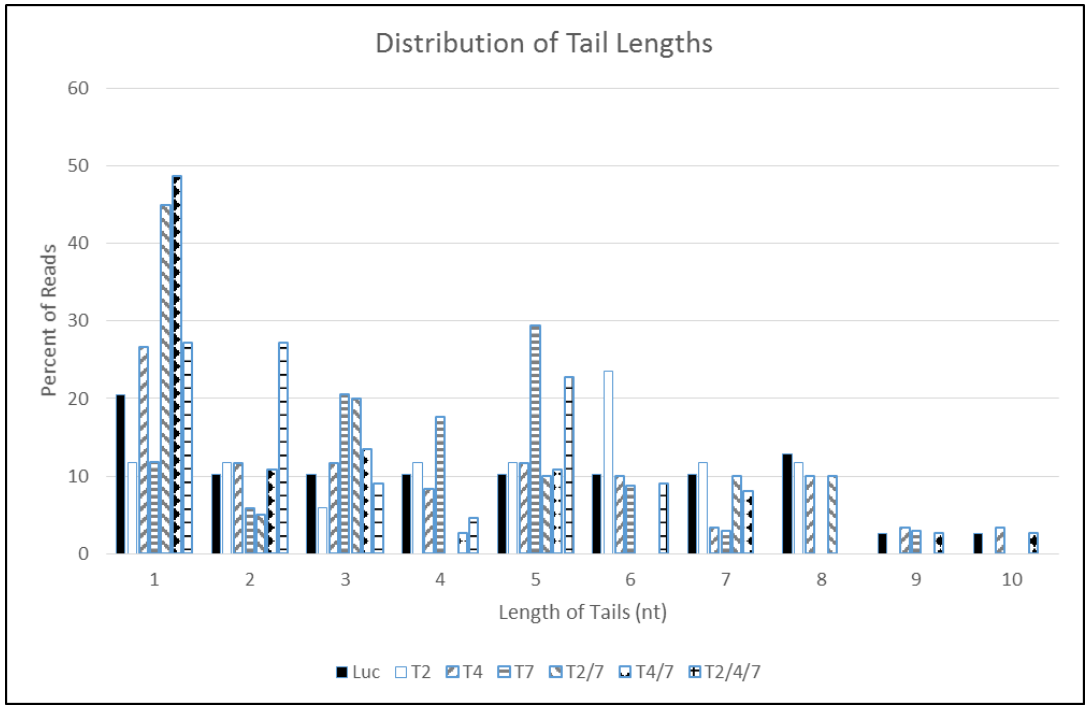

Figure 8. Sequencing of the 3' ends, Continued

G

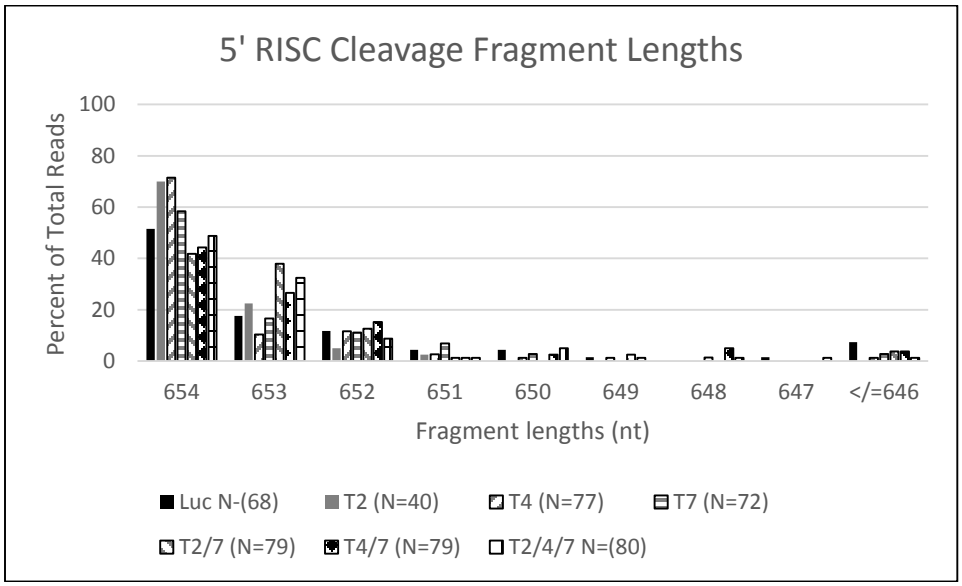

H

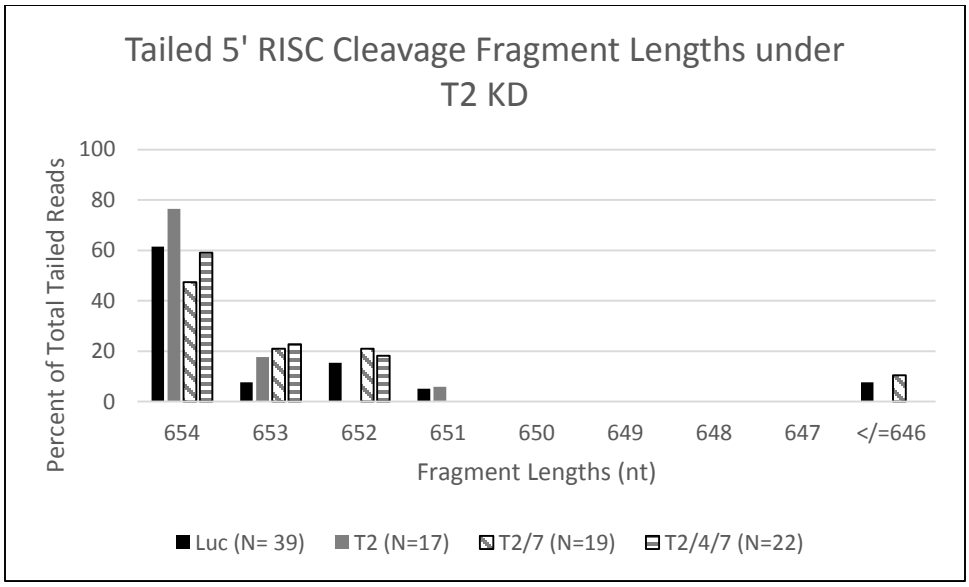

Figure 8. Sequencing of the 3' ends, Continued

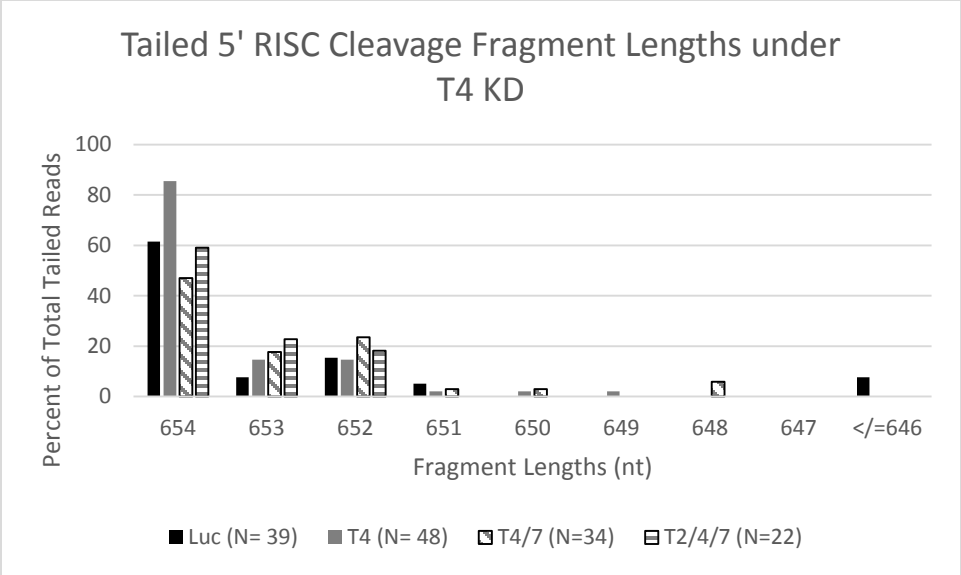

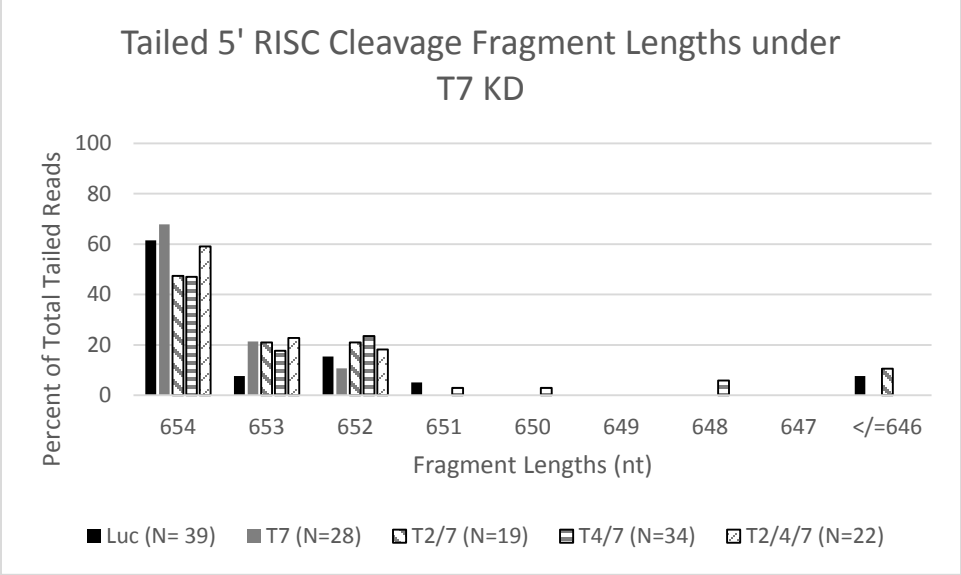

Figure 8. Sequencing of the 3' ends, Continued

I

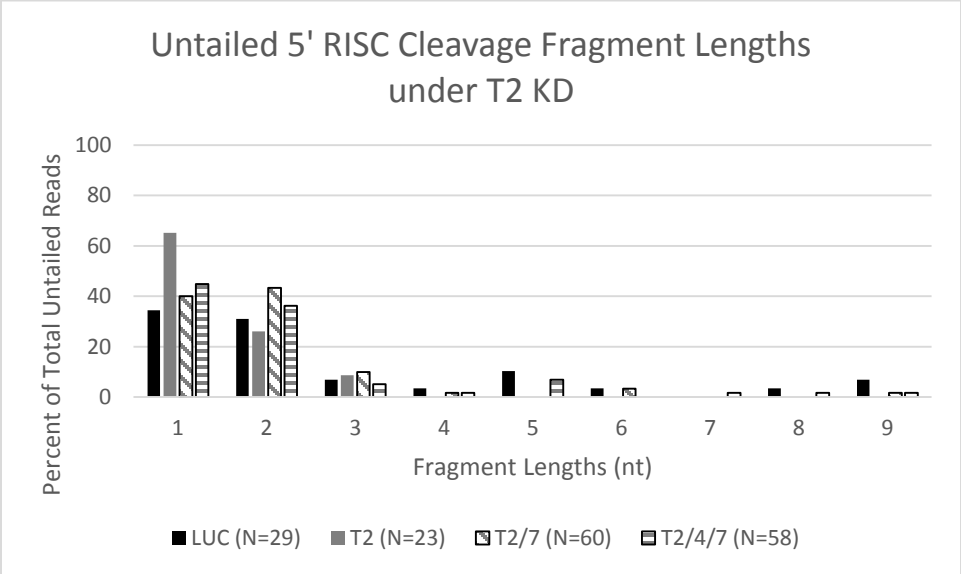

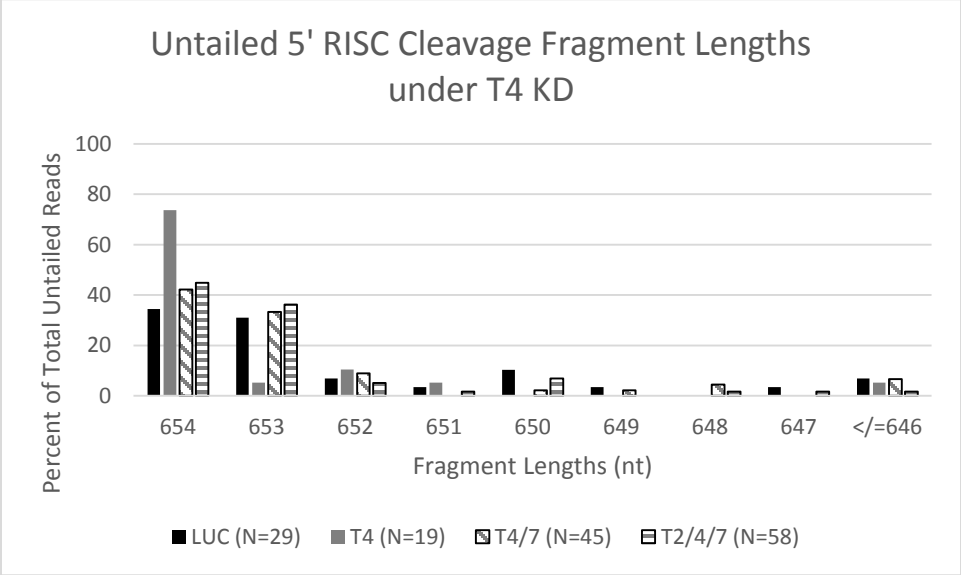

Figure 8. Sequencing of the 3' ends, Continued

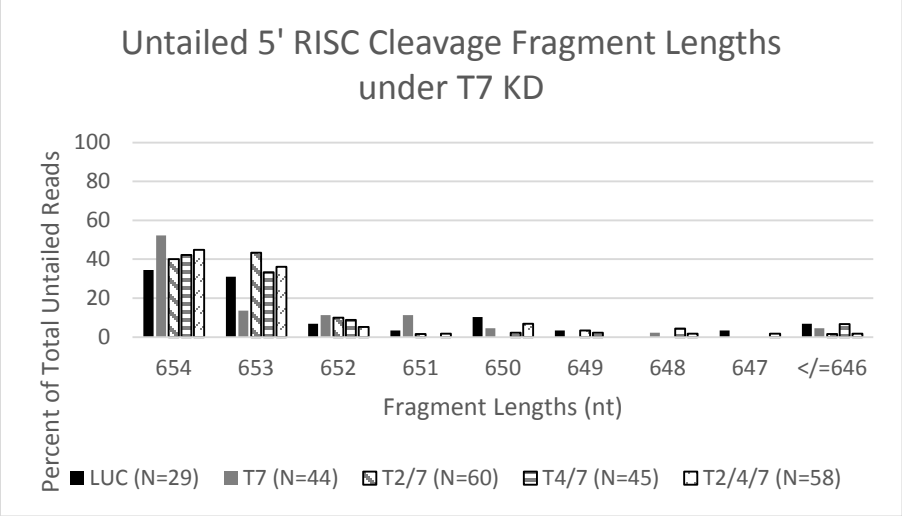

J

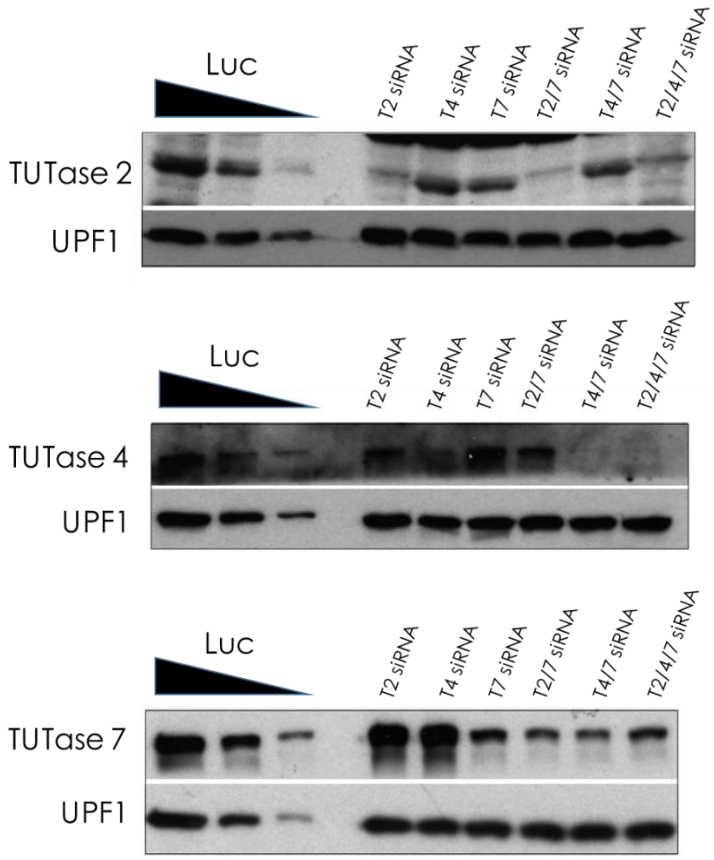

Figure 8. Sequencing of the 3' ends, Continued

Figure 9. RNA immunoprecipitation experiments reveal a physical interaction between TUTase 7 and the 5' RISC cleavage fragment of Bwt let-7.

(A) Schematic showing TUTase 4 DADA and TUTase 7 DADA mutants. Two conserved aspartic acid residues are mutated to alanines (D -> A).
(B) DADA mutant tailing assay. DADA mutants display significantly less activity.
(C) RIP experiment with TUTase 4, TUTase 7, and their respective DADA mutants. Bands corresponding to the full length reporter and the 5' RISC cleavage fragment are clearly indicated. The figure on the right is a darker exposure of the figure on the left.
(D) A repeat of the previous experiment with TUTase 7 and TUTase 7 DADA. Flag tag was used as a negative control. The lane containing the DADA mutant is labeled as T7D.
(E) Western blot of TUTase 7 expression in experiment (D).

A

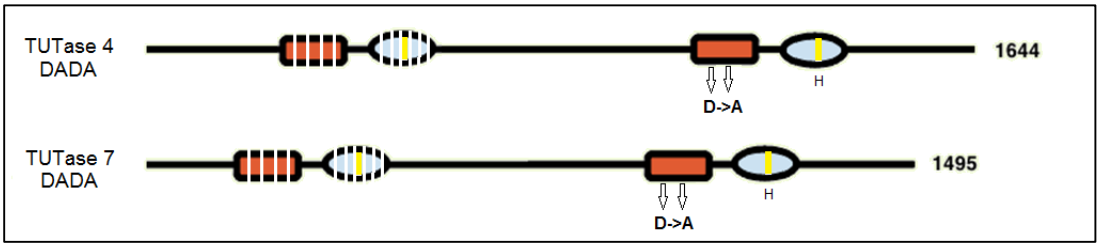

B

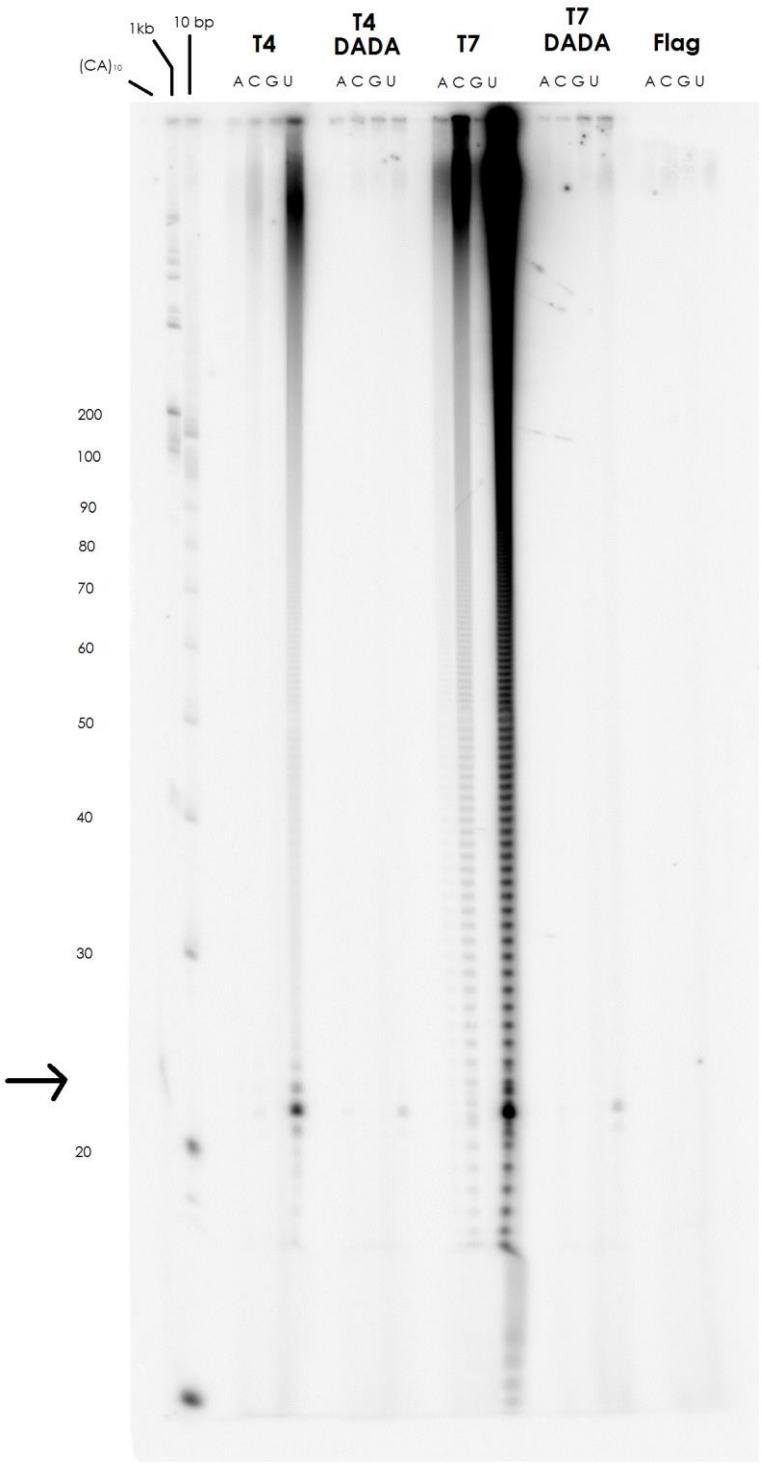

Figure 9. RNA immunoprecipitation experiments, Continued

C

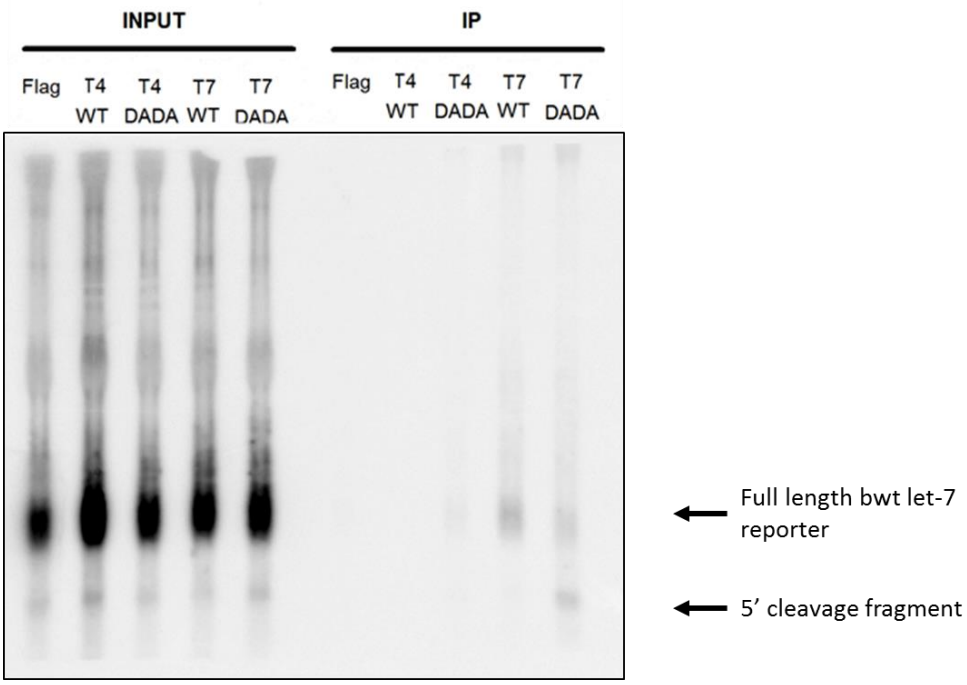

D

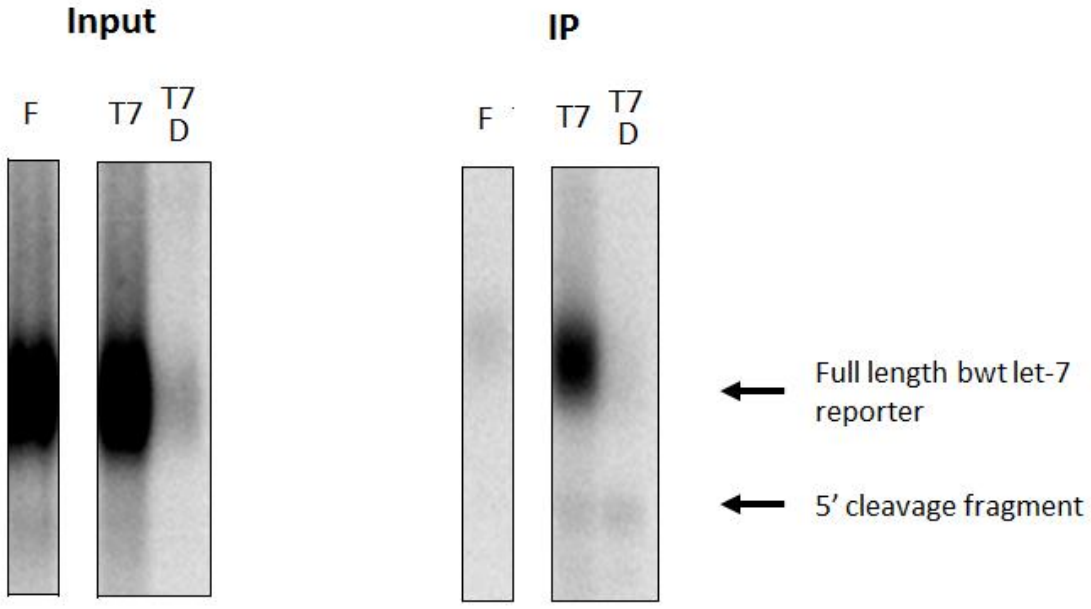

Figure 9. RNA immunoprecipitation experiments, Continued

E

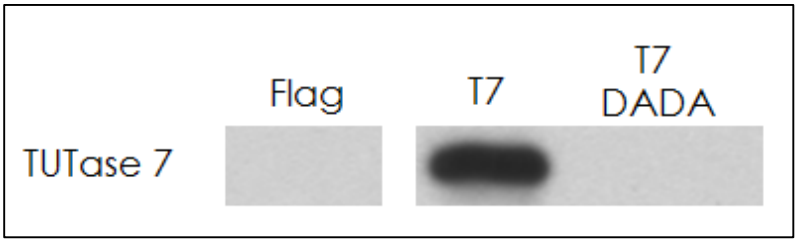

Figure 9. RNA immunoprecipitation experiments, Continued

Figure 10. Northern blot analysis of steady state levels of the Bwt let-7 reporter under various TUTase knockdown conditions.

(A) Northern blot probed with PC Delta 1,2 probe.
(B) Ratio of full length reporter to transfection control for (A)
(C) Ratio of the levels of 5' fragment to total levels of Bwt Let-7 reporter for (A)
(D) Western blots showing TUTase knockdowns for (A). UPF1 served as the loading control.
(E) Repeat experiment, probed with PTS(2) probe.
(F) Ratio of full length reporter to transfection control for (E)
(G) Ratio of the levels of 5' fragment to total levels of Bwt Let-7 reporter for (E)
(H) Western blots showing TUTase knockdowns for (E). UPF1 served as the loading control. * represents nonspecific bands.

A

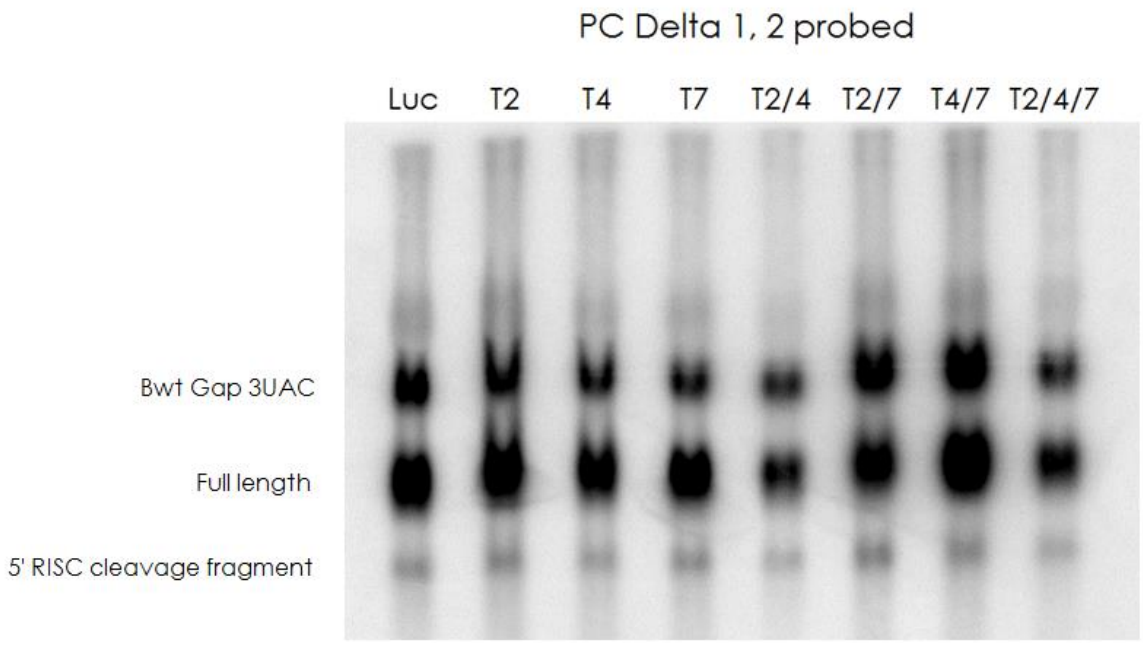
PC Delta 1, 2 probed
Luc
T2
T4
T7
T2/4
T2/7
T4/7
T2/4/7
Bwt Gap 3UAC
Full length
5' RISC cleavage fragment

B

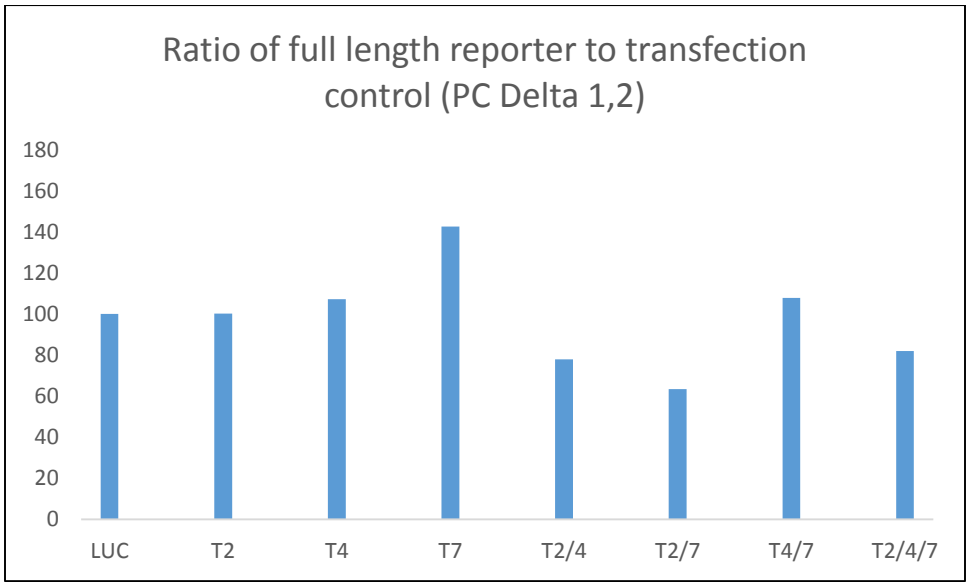
Ratio of full length reporter to transfection control (PC Delta 1,2)
180
160
140
120
100
80
60
40
20
0
LUC
T2
T4
T7
T2/4
T2/7
T4/7
T2/4/7

C

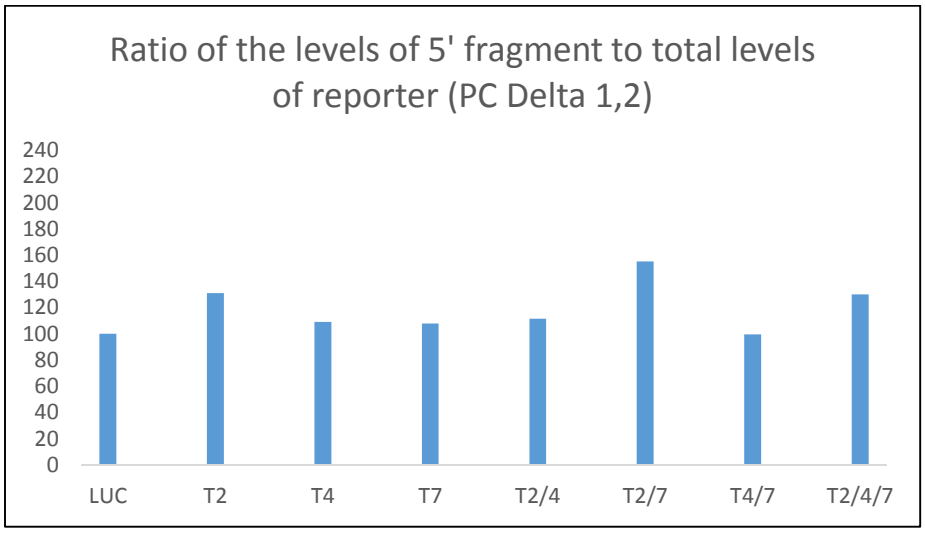

Figure 10. Northern blot analysis, Continued

D

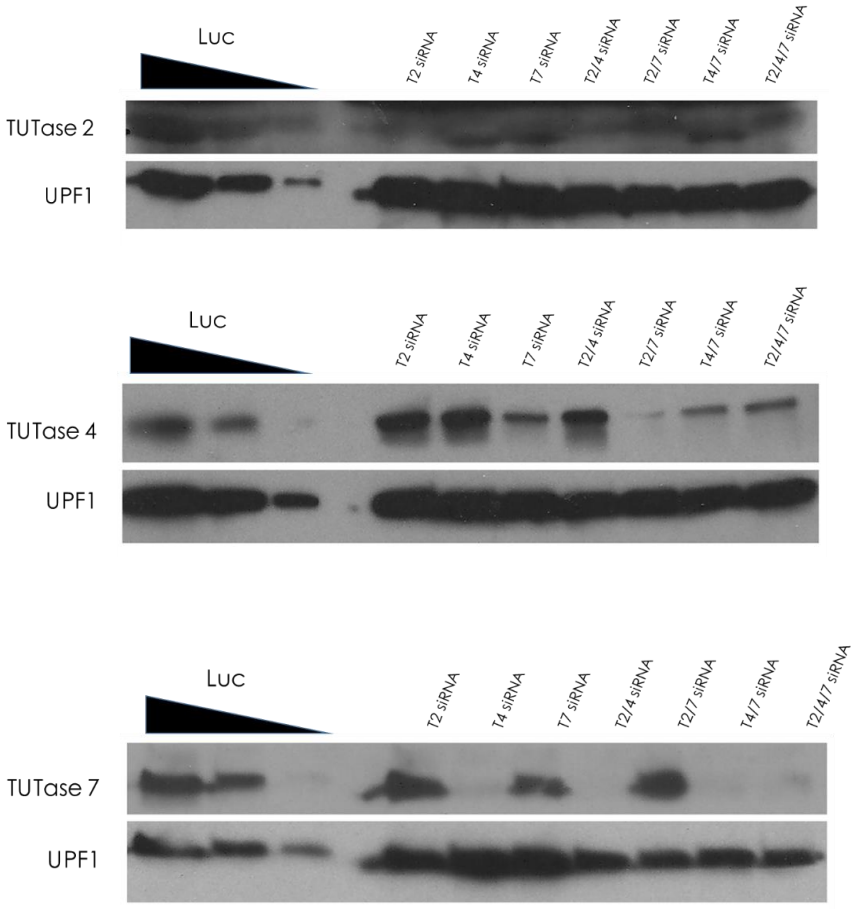

E

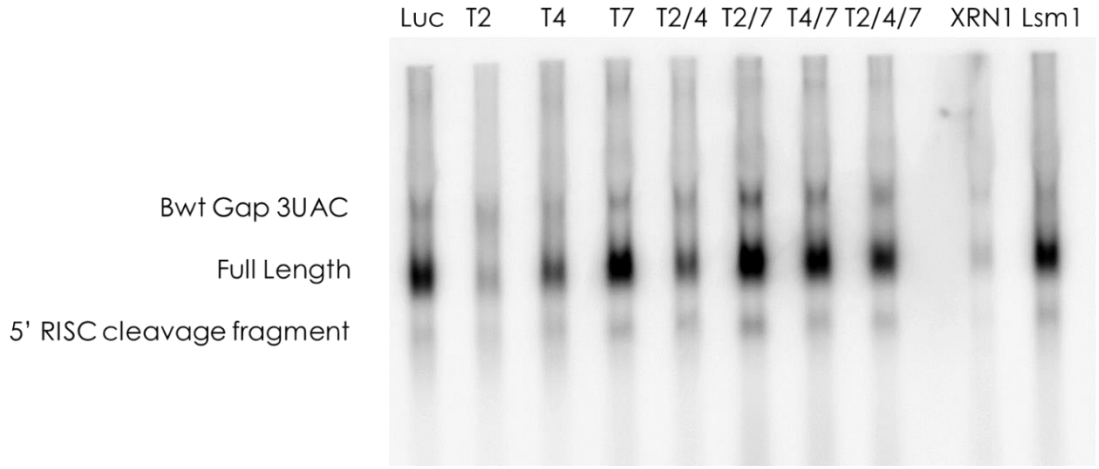

Figure 10. Northern blot analysis, Continued

F

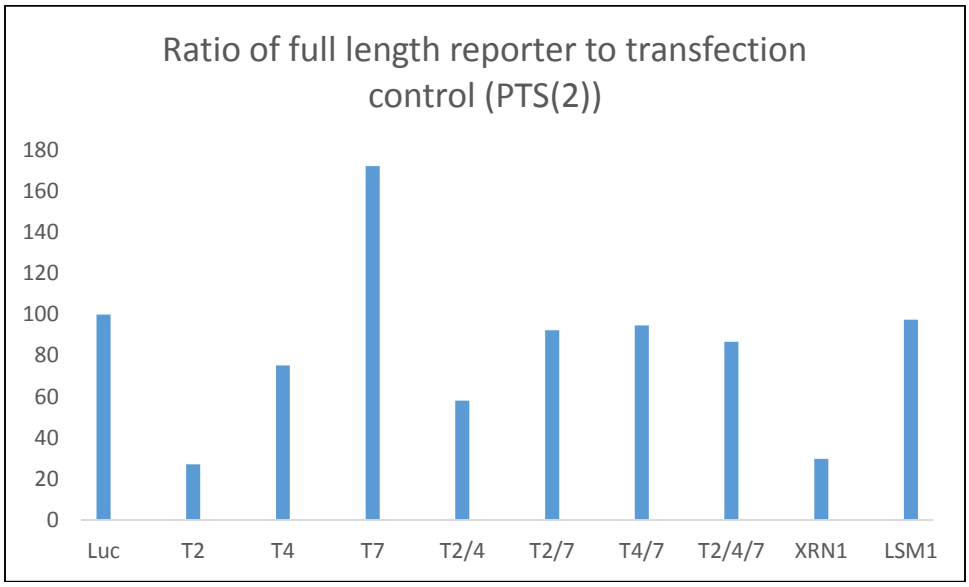

G

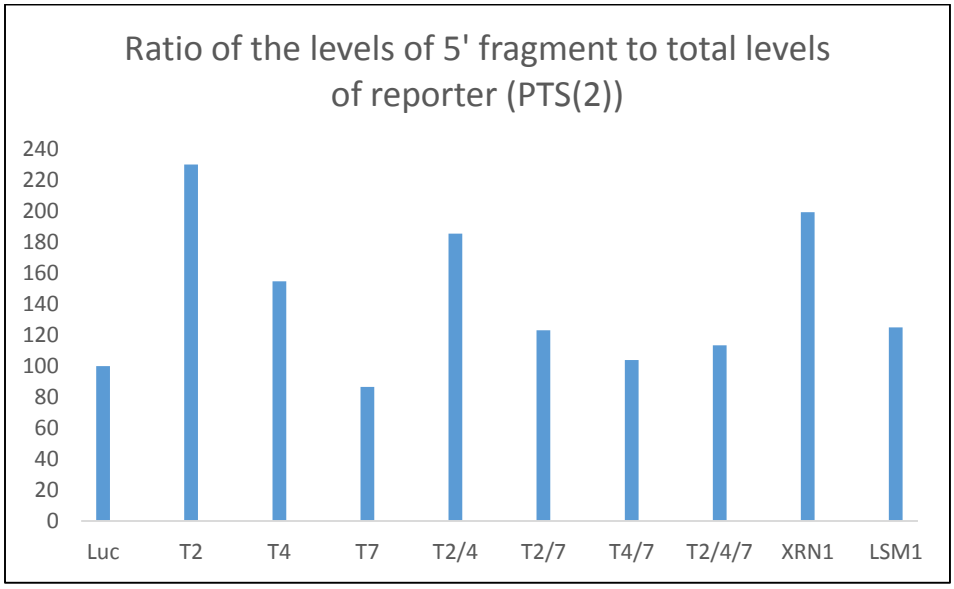

Figure 10. Northern blot analysis, Continued

H

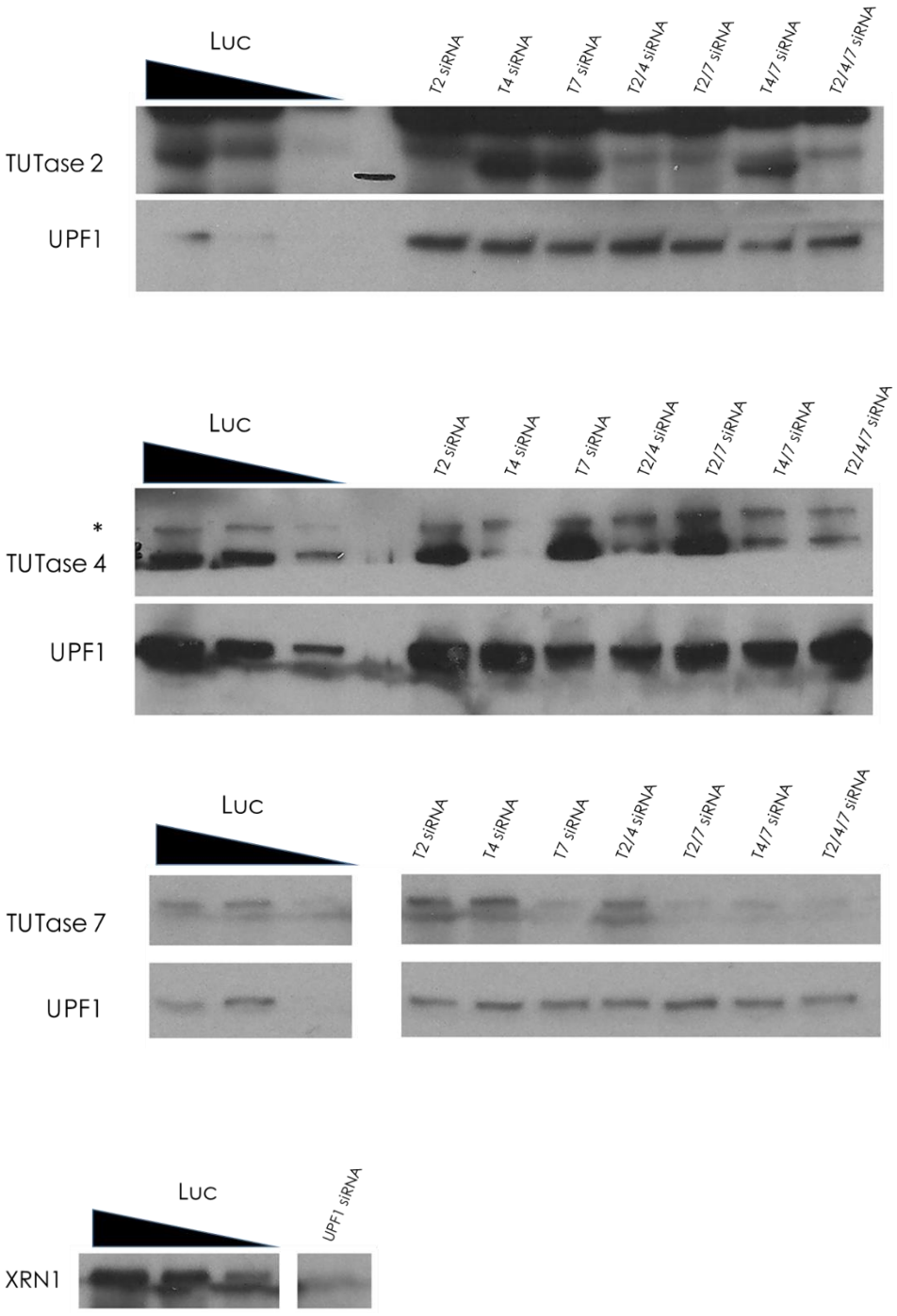

Figure 10. Northern blot analysis, Continued

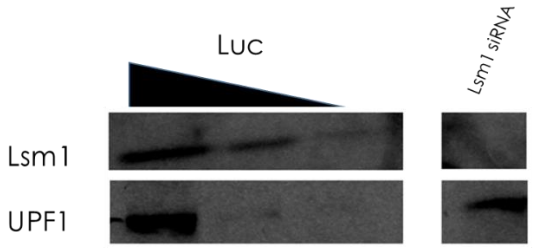

Figure 10. Northern blot analysis, Continued

III.

Discussion

Human TUTases exhibit differences in apparent tailing processivity and nucleotide preference *in vitro*

In this work, I have analyzed the activities and nucleotide preferences of six of the seven human non-canonical ribonucleotidyl transferases. Through in vitro tailing assays, I have shown that TUTase 4 and TUTase 7 have a strong preference for adding U residues to a synthetic CA_{10} RNA substrate. These results are in agreement with what has been found in previous reports (Norbury 2007; Heo et al. 2009). The Norbury group had observed uridylation by Cid1, the fission yeast ortholog of TUTase 7, on a synthetic A_{15} substrate. Heo et. al had observed uridylation of synthetic pre-let-7 miRNA by TUTase 4. Furthermore, TUTase 4 and 7 are the most active of the family. They were capable of catalyzing the addition of tails that were hundreds of nucleotides long. In contrast, TUTases 2, 3, 5 and 6 were only able to add single nucleotide tails. In vitro tailing experiments using both an A_{15} and a G_2U_{15} substrate have shown that TUTase 5 is a poly (A) polymerase, in agreement with our own data (Rammelt 2011). TUTase 2 and 3 also exhibited a preference in the addition of mono-A tails. However, under single nucleotide conditions, the nc-rNTrs exhibited an expanded range of activities, catalyzing the addition of a nontemplated tail using any of the nucleotides. These results indicate that in the absence of further data, there is the potential for individual TUTases/ncPAP family members to catalyze the addition of tails that are diverse in nucleotide composition.

TUTase 2 and 7 may collaborate in the oligouridylation of 5' RISC cleavage fragments

Sequencing results indicate that the U tails added to the 5' RISC cleavage fragment consist of predominantly uridine residues. Over half of all cloned fragments were found to carry 3' oligoU tails under the control conditions of luciferase siRNA treatment. Also, the average tail length was longest compared to the TUTase knockdown conditions.

Under a TUTase 2 and TUTase 7 knockdown, the percentage of transcripts tailed dropped to ~30%. This similar effect can also be seen under a TUTase 2, 4 and 7 combination knockdown. This decrease in tailed species suggests that TUTase 2 and 7 are responsible for uridylating the 5' RISC cleaved fragment. The implicated involvement of TUTase 2 in oligouridylation is of particular interest given existing literature on this enzyme, which has only described a role in polyadenylation of mRNAs or mono-uridylation of pre-miRNAs. Western blot data indicates that while the TUTase knockdowns were efficient, leading to approximately 11% of protein remaining, the residual proteins may be the reason a complete loss of tailing is not observed. A TUTase 2 knockdown alone failed to noticeably decrease the amount of tailed species. The same can be said about a lone TUTase 7 knockdown, leading to the conclusion that these two enzymes are possibly working redundantly. Interestingly, a TUTase 4 knockdown leads to an increase in the percentage of tailed transcripts. Currently, the reason for this is unknown, but may suggest a competition between TUTases in binding to target RNAs. The vast majority of tails are composed of uridines regardless of any

TUTase knockdowns. However, tail length analysis of tailed species revealed that knockdown of TUTases 4 and 7 leads to a decrease in the average lengths of the tails. Tail length distribution analysis revealed that a TUTase 2/7 combination knockdown leads to an increase in mono-tailed transcripts, suggesting that a decrease in the levels of TUTase 2 and 7 lead not only to less overall tailing, but also shorter tails. Furthermore, the distribution seen under a TUTase 4 knockdown was quite similar to the distribution of the luciferase control, suggesting TUTase 4 may have little to no impact on determining the length of tails. Fragment length analysis reveals that the knockdown of any TUTase results in a change in the preferential position of tailing. While single knockdowns led to an increase in the occurrence of full length transcripts, combination knockdowns led to a decrease. The reason for this difference is currently unclear. However, all three TUTases seem to have an impact on determining the position of tailing. Outstanding questions raised by our findings is how TUTase 2, a nc-rNTRs with adenosine preference, contributes oligouridylation, how the TUTases are directed to 5' RISC cleaved mRNAs for tailing, and whether cofactors act to stimulate or limit the processivity of the tailing enzyme(s) in a manner analogous to Lin28 in TUTase 4-dependent pre-miRNA oligouridylation or RNA helicase Mtr4 in TRAMP-dependent oligoadenylation (Yeom 2011; Jia 2011)

We note that the results presented here are from a single set of knockdowns, and should therefore be considered preliminary. More biological repeats of this data will be necessary to confidently identify TUTase 2 and 7 as the enzymes responsible for uridylating the 5' RISC cleavage fragment.

TUTase 7 may directly contribute to the oligouridylation of 5' RISC cleaved fragments through physical association

The results from sequencing suggested that TUTase 7 is at least partly responsible for uridylating the 5' RISC cleavage fragment. Our preliminary data revealed an enriched association between the TUTase 7 DADA mutant and the 5' RISC cleavage fragment over the full length B-let7 mRNA, compared to the wild type protein. These data support a direct role for TUTase 7 in the binding of B-let7 mRNA and tailing of 5' RISC-cleaved mRNAs. These results are consistent with our sequencing data in supporting a model in which TUTase 7 catalyzes uridylation of the 5' RISC cleavage fragment. Repeats of the RIP experiments with normalized protein expression levels are needed to directly compare TUTase 4 and TUTase 7 interactions with the full-length and 5' RISC-cleaved reporter mRNAs. Based on our sequencing data, we anticipate that catalytically inactive mutants of TUTase 4 will not exhibit the enrichment of 5' RISC cleavage fragments observed with TUTase 7. Furthermore, the addition of catalytically inactive mutants of TUTase 2 to this experiment will be an important complement to the results seen in the sequencing data. From our data, we suspect TUTase 2 is involved in directly tailing the 5' RISC cleavage fragment, and therefore we anticipate being able to detect a physical interaction between the two.

Future directions for this work

Much remains to be understood regarding 3' end tailing as an RNA modification in post-transcriptional gene regulation. Our work outlines a relatively simple approach to detecting and characterizing 3' tails on specific RNA transcripts. It will be interesting to determine if recently identified endogenous targets of miRNA-directed RISC (or other endonuclease) cleavage also undergo oligouridylation or other RNA tailing. Our finding that catalytically inactive Tutases may preferentially stabilize interactions with RNA targets leaves us poised to identify additional, currently unknown classes of mRNA or non-coding RNA tailing targets. In fact, recent proteomics work characterizing mRNP composition in mammalian cells identified both TUTase 4 and TUTase 7, suggesting that at least some polyadenylated mRNA species are targeted for tailing by TUTases (Castello 2012).

Our identification of at least two TUTases responsible for the oligouridylation of the 5' RISC cleavage fragment of Bwt let-7 mRNA gives us a tool for further dissection of both the upstream pathways that lead to TUTase recruitment and the downstream impact of oligouridylation on RISC cleaved mRNA metabolism. The efforts described here in analyzing the downstream impacts of tailing on RNA decay may have been limited by use of steady state measurements rather than pulse-chase decay assays. Our preliminary data suggests that 5' RISC-cleaved fragments undergo decay in a manner at least partially dependent on Lsm1. This conclusion, along with suggestion that RISC cleavage is promoted under Xrn1 depletion (perhaps reflecting stabilization of mature let-7), awaits confirmation through biological repeats. Of additional

interest is whether the 5' RISC-cleaved fragment undergoes translational repression or Dis3l2-dependent decay, given the existing work suggesting such downstream impacts for oligouridylation on other RNA transcripts.

Together, these future research efforts based on the work described here for a model target of oligouridylation, the 5' RISC-cleaved mRNA, are expected to lend greater insight into the importance of this fascinating and highly conserved RNA modification.

IV.

Materials and Methods

Adapter-ligation mediate reverse transcription-PCR

Total RNA was isolated from HeLa cells using TRIzol® reagent. The RNA was DNase treated, phosphatase treated, and an adaptor was ligated onto the 3' ends. One of two primers were used for reverse transcription, U-specific or unbiased. The resulting cDNA was PCR amplified using a gene specific Bwt forward primer and an adaptor specific reverse primer. The PCR reaction was run on a 1.5% ethidium bromide stained agarose gel and imaged.

Protein immunoprecipitation and RNA immunoprecipitation

3X Flag tagged TUTase constructs were transfected into HEK 293T cells via TransIT®-293 transfection reagent. Cells were lysed and incubated with Anti-Flag agarose beads (Sigma-Aldrich). For protein immunoprecipitations, cell extracts were RNase A treated. The 3X Flag tagged TUTases were eluted from the beads with the addition of an excess amount of 3X Flag peptide. The eluted proteins were frozen down in elution buffer and stored at -80 degrees. Western blot analysis for relative protein concentrations is outlined below. For RNA immunoprecipitations, TRIzol® reagent was added directly to the beads after incubation with cell lysate. RNA was isolated and used for Northern blot analysis.

GST-Flag protein normalization for tailing assays

After purification of the TUTases, each preparation was loaded onto an 8% SDS-PAGE gel followed by Western blot analysis using rabbit anti-Flag antibody. The concentrations of purified TUTase preps were determined by comparing the intensities of detected bands against a titration of GST-Flag protein.

In vitro RNA tailing assays

Tailing assays under physiological NTP concentrations were carried out in 25 µl reaction mixtures containing 150nM final concentration of purified proteins and 500 pmol of the $(CA)_{10}$ RNA substrate. Non-physiological, single nucleotide reaction conditions contained only a single nucleotide. To visualize tailing products bearing a particular nucleotide, a 32P-labeled nucleotide was included. Reactions were initiated by addition of the purified nc-rTRs being assayed, incubated for 45 minutes at 37 degrees, and stopped by the addition of EDTA. Comparative analysis of different nc-rTRs in a given assay was performed using similar amounts of purified enzymes as judged by protein normalization (described above). The RNA was precipitated, and a formamide loading buffer was used to resuspend the RNA pellets. The resuspended pellets were denatured at 95 degrees for 2 minutes and separated on a 10% polyacrylamide/Urea denaturing gel, using 5' 32P-endlabeled $(CA)_{10}$ RNA substrate and DNA molecular weight markers as length markers. A PhosphorImager was used to image radioactive reaction products.

siRNA transfections for TUTase knockdowns

Knockdowns of the TUTases using siRNAs were done in HeLa tet-off cells. At approximately 30% confluency, cells were transfected with siRNAs targeting the TUTases using Silentfect™ transfection reagent. At approximately 80% confluency, a second transfection using Lipofectamine® 2000 reagent was performed. siRNAs targeting the TUTases and a tet-inducible Bwt let-7 reporter were simultaneously transfected. Tetracycline was added to the media prior to

prevent expression of the Bwt let-7 reporter. 10 hours before cell harvest, tetracycline was removed from the media to allow expression of the reporter. Cells were harvested using TRIzol® reagent. One set of cells for each knockdown condition was harvested in 2X SDS page buffer for protein analysis. Knockdown efficiencies were measured using western blot analysis. The TUTase 2, TUTase 4, and TUTase 7 antibodies were acquired from Abcam (ab103884), Abcam (ab89165), and Sigma-Aldrich (SAB1400699) respectively.

Cloning and sequencing

Total RNA was isolated from HeLa Tet-Off cells using TRIzol® reagent. The RNA was DNase treated, phosphatase treated, and an RNA adapter containing a barcode was ligated to the 3' ends. The 5' end of the RNA adapter contained a dinucleotide barcode, followed by a 4 nucleotide randomer. A gene specific Bwt forward primer and an adaptor specific reverse primer were used to PCR amplify the reporter. The PCR product was run on a 1.5% ethidium bromide stained agarose gel. The band corresponding to the 5' RISC cleavage fragment was extracted and ligated into the TOPO® cloning vector. The ligation product was then transformed into TOP10 competent *E. coli* cells and plated on agar plates containing kanamycin. Positive colonies were picked and cultured for Qiagen Miniprep plasmid purification. The resultant DNA plasmids were sequenced using the M13F primer. Sequence alignments were done using AlignX® software. Sequences were aligned against the Bwt let-7 reporter, and nucleotides deviating from the Bwt let-7 sequence at and before the cleavage site were interpreted as untemplated tails. Each knockdown condition was

previously assigned a unique dinucleotide barcode during the adaptor ligation step and sequences were organized according to their barcode. The 4 nucleotide randomer allowed for the identification of duplicate sequences that arose as a result of PCR amplification. Sequences with identical dinucleotide barcodes, 4 nucleotide randomers, tails, and cleavage site were considered duplicate sequences. Duplicate sequences were altogether counted as a single read.

Northern blot analysis

The Bwt let-7 reporter and the Bwt Gap 3'UAC reporters used in the Northern blot experiments were expressed under a CMV promoter. HeLa Tet-Off cells were transfected with siRNAs targeting the TUTases, the Bwt let-7 reporter, and Bwt Gap 3'UAC reporter using the conditions described above. Tetracycline was not added to the media. Cells were harvested in TRIzol® reagent, with one set for each condition harvested in SDS page buffer for protein analysis. RNA was isolated and resuspended in formamide loading buffer. The samples were run on a formaldehyde/agarose gel and transferred to a membrane. The membrane was incubated with a radioactive probe and exposed to a phosphor screen. A PhosphorImager was used to image radioactive reaction products.

References

Berndt, H., Harnisch, C., Rammelt, C., Stohr, N., Zirkel, A., Dohm, J.C., Himmelbauer, H., Tavanez, J., Huttelmaier, S. and Wahle, E. Maturation of mammalian H/ACA box snoRNAs: PAPD5-dependent adenylation and PARN-dependent trimming. RNA 18, 958-72 (2012).

Burns, D.M., D'Ambrogio, A., Nottrott, S., Richter, J.D., CPEB and two poly(A) polymerases control miR-122 stability and p53 mRNA translation. Nature 473, 105-8 (2011).

Callahan, K.P., Butler, J.S., TRAMP complex Enhances RNA Degradation by the Nuclear Exosome Component Rrp6. J Biol Chem 285, 3540-3547 (2010).

Castello, A., Fischer, B., Eichelbaum, K., Horos, R., Beckmann, B.M., Strein, C., Davey, N.E., Humphreys, D.T., Preiss, T., Steinmetz, L.M., Krijgsveld, J., Hentze, M.W., Insights into RNA biology from an atlas of mammalian mRNA-binding proteins. Cell 149, 1393-406 (2012).

Chang, H.M., Triboulet, R., Thornton, J.e., Gregory, R.I., A role for the Perlman syndrome exonuclease Dis3l2 in the Lin28-let-7 pathway. Nature 0, 1-7 (2013)

Choi, Y.S., Patena, W., Leavitt, A.D., McManus, M.T., Widespread RNA 3'-end oligouridylation in mammals. RNA 18, 394-401 (2012).

D'Ambrogio, A., Gu, W., Udagawa, T., Mello, C.C., Richter, J.D., Specific miRNA Stabilization by Gld2-Catalyzed Monoadenylation. Cell Rep 2, 1537-45 (2012).

Dominski, Z., Marzluff, W.F., Formation of the 3' end of histone mRNA. Gene 239, 1-4 (1999)

Gallouzi, I.E., Wilusz, J., A DIStinctively novel exoribonuclease that really likes U. EMBO J 32, 1799-801 (2013).

Garneau, N.L., Wilusz, J., Wilusz, C.J., The highways and byways of mRNA decay. Nat Rev Mol Cell Biol 8, 113-26 (2007)

Hagan, J.P., Piskounova, E., Gregory, R.I., Lin28 recruits the TUTase Zcchc11 to inhibit let-7 maturation in mouse embryonic stem cells. Nat Struct Mol Biol, 10, 1021-5 (2009).

Heo, I., Joo, C., Kim, Y.K., Ha, M., Yoon, M.J., Cho, J., Yeom, K.H., Han, J., Kim, V.N., TUT4 in Concert with Lin28 Suppresses MicroRNA Biogenesis through Pre-MicroRNA Uridylation. Cell 138, 696-708 (2009).

Heo, I., Ha, M., Lim, J., Yoon, M.J., Park, J.E., Kwon, S.C., Chang, H., Kim, V.N., Mono-Uridylation of Pre-MicroRNA as a Key Step in the Biogenesis of Group II let-7 MicroRNAs. Cell 151, 521-32 (2012).

Hoefig, K.P., Rath, N., Heinz, G.A., Wolf, C., Dameris, J., Schepers, A., Kremmer, E., Ansel, K.M., Heissmeye, V. Eri1 degrades the stem-loop of oligouridylated histone mRNAs to induce replication-dependent decay. Nat Struct Mol Biol 20, 73-83 (2013).

Houseley, J., LaCava, J., Tollervey, D., RNA-quality control by the exosome. Nat Rev Mol Cell Biol 7, 529-39 (2006).

Katoh, T., Sakaguchi, Y., Miyauchi, K., Suzuki, T., Kashiwabara, S., Baba, T., Suzuki, T., Selective stabilization of mammalian microRNAs by 3' adenylation mediated by the cytoplasmic poly(A) polymerase GLD-2. Genes Dev 23, 433-8 (2009).

Kwak, J.E., Wickens, M., A family of poly (U) polymerases. RNA 13, 860-867 (2007).

Jia, H., Wang, X., Liu, F., Guenther, U.P., Srinivasan, S., Anderson, J.T., Jankowsky, E., The RNA helicase Mtr4p modulates polyadenylation in the TRAMP complex. Cell 145, 890-901 (2011).

Lapointe, C.P., Wickens, M., The Nucleic Acid-binding Domain and Translational Repression Activity of a Xenopus Terminal Uridylyl Transferase. J Biol Chem 288, 20723-20733 (2013).

Lee, S.R., Lykke-Andersen, J., Emerging roles for ribonucleoprotein modification and remodeling in controlling RNA fate. Trends Cell Biol 969, 1-7 (2013).

Lehrbach, N.M., Armisen, J., Lightfoot, H.L., Murfitt, K.J., Bugaut, A., Balasubramanian, S., Miska, E.A., Lin-28 and the poly(U) polymerase PUP-2 regulate let-7 microRNA processing in Caenorhabditis elegans. Nat Struct Mol Biol 10, 1016-20 (2009).

Lubas, M., Christensen, M.S., Kristiansen, M.S., Domanski, M., Falkenby, L.G., Lykke-Andersen, S., Andersen, J.S., Dziembowski, A. and Jensen, T.H. Interaction profiling identifies the human nuclear exosome targeting complex. Mol Cell 43, 624-37 (2011).

Lunde, B.M., Magler, I., Meinhart, A., Crystal structures of the Cid1 poly (U) polymerase reveal the mechanism for UTP selectivity. Nucleic Acids Res 40, 9815-24 (2012).

Malecki, M., Viegas, S.C., Carneiro, T., Golik, P., Dressaire, C., Ferreira, M.G., Arraiano, C.M., The exoribonuclease Dis3l2 defines a novel eukaryotic RNA degradation pathway. EMBO J 32, 1842-54 (2013).

Martin, G. and Keller, W. RNA-specific ribonucleotidyl transferases. RNA 13, 1834-49 (2007).

Mellman, D.L., Gonzales, M.L., Song, C., Barlow, C.A., Wang, P., Kendziorski, C. and Anderson, R.A. A ptdIns4,5P2-regulated nuclear poly(A) polymerase controls expression of select mRNAs. Nature 451, 1013-7 (2008).

Morozov, I.Y., Meriel, G.J., Gould, P.D., Crome, V., Wilson, J.B., Hall, A.J.W., Rigden, D.J., Caddick, M.X., mRNA 3' Tagging is induced by nonsense-mediated decay and promotes ribosome dissociation. Mol Cell Biol 32, 2585-95 (2012).

Morris, M.R., Astuti, D., Maher, E.R., Perlman Syndrome: Overgrowth, Wilms Tumor Predisposition and DIS3l2. Am J Med Genet C Semin Med Genet 163, 106-13 (2013).

Mullen, T.E. and Marzluff, W.F. Degradation of histone mRNA requires oligouridylation followed by decapping and simultaneous degradation of the mRNA both 5' to 4" and 3' to 5'. Genes Dev 22, 50-65 (2008).

Munoz-Tello, P., Gabus, C., Thore, S., Functional implications from the Cid1 poly(U) polymerase crystal structure. Structure 20, 977-86 (2012).

Nakanish, T., Kubota, H., Ishibashi, N., Kumagai, S., Watanabe, H., Yamashita, M., Kashiwabara, S., Miyado, K. and Baba, T. Possible role of mouse poly(A) polymerase mGLD-2 during oocyte maturation. Dev Biol 289, 115-26 (2006).

Nagaike, T., Suzuki, T., Katoh, T. and Ueda, T. Human mitochondrial mRNAs are stabilized with polyadenylation regulated by mitochondria-specific pol(A) polymerase and polynucleotide phosphorylase. J Biol Chem 280, 19721-27 (2005).

Norbury, C.J. 3' uridylation and the regulation of RNA function in the cytoplasm. Biochem Soc Trans 38, 1150-3 (2010).

Rammelt, C., Bilen, B., Zavolan, M. and Keller, W. PAPD5, a noncanonical poly(A) polymerase with an unusual RNA-binding motif. RNA 9, 1734-46 (2011).

Rissland, O.S., Mikulasova, A. and Norbury, C.J. Efficient RNA polyuridylation by noncanonical poly(A) polymerases. Mol Cell Biol 27, 3612-24 (2007).

Schmidt, K., Butler, J.S., Nuclear RNA surveillance: role of TRAMP in controlling exosome specificity. Wiley Interdiscip Rev RNA 4, (217-31) (2013).

Schmidt, M.J., Norbury, C.J., Polyadenylation and beyond: emerging roles for noncanonical poly (A) polymerases. Wiley Interdiscip Rev RNA 1, 142-51 (2010).

Schmidt, M.J., West, S. and Norbury, C.J. The human cytoplasmic RNA terminal U-transferase ZCCHC11 targets histone mRNAs for degradation. RNA 17, 39-44 (2011).

Scott, D.D., Norbury, C.j., RNA decay via 3' uridylation. Biochim Biophys Acta 1829, 654-65 (2013).

Sement, F.M., Ferrier, E., Zuber, H., Merret, R., Alioua, M., Deragon, J.M., Cecile, B.A., Lange, H., Gagliardi, D., Uridylation prevents 3' trimming of oligoadenylated mRNAs. Nucleic Acids Res 41, 7115-7127 (2013).

Shatkin, A.J., Manley, J.L., The ends of the affair: Capping and polyadenylation. Nat Struct Biol 7, 838-42 (2000).

Shcherbik, N., Wang, M., Lapik, Y.R., Srivastava, L. and Pestov, D. Polyadenylation and degradation of incomplete RNA polymerase I transcripts in mammalian cells. Embo J 11, 106-11 (2010).

Shen, B. and Goodman, H.M. Uridine addition after microRNA-directed cleavage. Science 306, 997 (2004).

Song, M.G., Kiledjian, M., 3' Terminal oligo U-tract-mediated stimulation of decapping. RNA 13, 2356-65 (2007).

Su, W., Slepenkov, S.V., Slevin, M.K., Lyons, S.M., Ziemniak, M., Kowalska, J., Darzynkiewicz, E., Jemielity, J., Marzluff, W.F., Rhoads, R.E., mRNAs containing the histone 3' stem-loop are degraded primarily by decapping mediated by oligouridylation of the 3' end. RNA 19, 1-16 (2013).

Thornton, J.E., Chang, H.M., Piskounova, E., Gregory, R.I., Lin28-mediated control of let-7 microRNA expression by alternative TUTases Zcchc11 (TUT4) and Acchc6 (TUT7). RNA 18, 1875-85 (2012).

Trippe, R., Guschina, E., Hossbach, M., Urlaub, H., Luhrmann, R. and Benecke, B. Identification, cloning, and functional analysis of the human U6 snRNA-specific terminal uridylyl transferase. RNA 8, 1494-504 (2006).

Traut, T.W. Physiological concentrations of purines and pyrimidines. Mol Cell Biochem 140, 1-22 (1994).

Tharun, S., He, W., Mayes, A.E., Lennertz, P., Beggs, J.D., Parker, R., Yeast Sm-like proteins function in mRNA decapping and decay. Nature 30, 515-8 (2000).

Wilusz, C.J. & Wilusz, J. New ways to meet your (3') end—oligouridylation as a step on the path to destruction. Genes Dev 22, 1-7 (2008).

Wilusz, J.E., JnBaptiste, C.K., Lu, L.Y., Kuhn, C.D., Joshua-Tor, L., Sharp, P.A., A triple helix stabilizes the 3' ends of long noncoding RNAs that lack poly(A) tails. Genes Dev 26, 2392-2407 (2012).

Wyman, S.K., Knouf, E.C., Parkin, R.K., Fritz, B.R., Lin, D.W., Dennis, L.M., Krouse, M.A., Webster, P.J., Tewari, M., Post-transcriptional generation of miRNA variants by multiple nucleotidyl transferases contributes to miRNA transcriptome complexity. Genome Res 21, 1450-1461 (2011).

Yates, L.A., Fleurdepine, S., Rissland, O.S., De Colibus, L., Harlos, K., Norbury, C.J., Gilbert, R.J., Structural basis for the activity of a cytoplasmic RNA terminal uridylyl transferase. Nat Struct Mol Biol 19 782-7 (2012).

Yates, L.A., Norbury, C.J., Gilbert, R.J.C., The Long and Short of MicroRNA. Cell 153, 516-519 (2013).

Yeom, K.H., Heo, I., Lee, J., Hohnq, S., Kim, V.N., Joo, C., Single-molecule approach to immunoprecipitated protein complexes: insights into miRNA uridylation. EMBO Rep 12, 690-6 (2011).